HR-LCMS profiling, in vitro and in silico assessment of the antibacterial activities of endophytic Bacillus amyloliquefaciens NWR-14 from Piper chaba W. Hunter

Asokan, S.; Jacob, T.; Cherian, T.; Merlin, T.; Vivekanandhan, S.; AlSosowaa, A.A.; ... ; Vijayan, S.

Phytomedicine Plus 5 (2025) 100885

Contents lists available at ScienceDirect

Phytomedicine Plus

journal homepage: www.sciencedirect.com/journal/phytomedicine-plus

HR-LCMS profiling, in vitro and *in silico* assessment of the antibacterial activities of endophytic *Bacillus amyloliquefaciens* NWR-14 from *Piper chaba* W. Hunter

Sijo Asokan [a], Teena Jacob [b], Tijo Cherian [c], Teena Merlin [a], Vivekanandhan S [d], Afaf A AlSosowaa [a], Mostafa Mohammed Atiyah [a], Faheem Q Al-Mojahid [a], Willie J.G.M. Peijnenburg [e], Smitha Vijayan [a,*]

[a] School of Biosciences, Mar Athanasios College for Advanced Studies Tiruvalla, Pathanamthitta, Kerala, India
[b] Department of Microbiology, Pushpagiri Institute of Medical Sciences and Research Centre, Tiruvalla, Kerala, India
[c] Post Graduate Department of Food and Industrial Microbiology, Bishop Kurialacherry College for Women, Amalagiri, Kottayam 686561, Kerala, India
[d] Department of Microbiology, K.S.R College of Arts and Science for Women, Tiruchengode, Tamil Nadu, India
[e] Institute of Environmental Sciences (CML), Leiden University, Leiden, Netherlands

ARTICLE INFO

Keywords:
Endophytic bacteria
Piper chaba
Bacillus amyloliquifaciens
ESBL Klebsiella pneumoniae
Antibacterial activity
Antibiofilm activity

ABSTRACT

Background: The rise of multidrug-resistant (MDR) pathogens such as *Klebsiella pneumoniae*, particularly those producing extended-spectrum β-lactamases (ESBL), has intensified the search for novel bioactive compounds. Medicinal plants, including *Piper chaba*, host endophytic bacteria that may serve as promising sources of antimicrobial agents.

Purpose: This study aimed to evaluate the antibacterial, antibiofilm, antioxidant, and cytotoxic properties of secondary metabolites derived from *Bacillus amyloliquefaciens* NWR-14, an endophyte isolated from *P. chaba*, with a focus on its activity against ESBL-producing *K. pneumoniae*.

Methods: B. amyloliquefaciens NWR-14 was isolated and identified via 16S rRNA gene sequencing. The ethyl acetate extract of this isolate was tested for antibacterial activity using MIC and MBC assays. Antibiofilm potential was assessed using crystal violet staining. Scanning electron microscopy (SEM) was employed to visualize morphological changes in *K. pneumoniae*. HR-LCMS was used to putatively annotate bioactive compounds. *In silico* molecular docking was conducted to assess binding affinities to the CTX-M-15 β-lactamase enzyme. Antioxidant activity was evaluated using DPPH, FRAP, and ABTS assays, and cytotoxicity was tested on fibroblast cells.

Results: The extract exhibited notable antibacterial activity with a MIC and MBC of 1.56 mg/mL, and showed dose-dependent biofilm inhibition, achieving maximum effect at 6 mg/mL. SEM analysis confirmed significant cellular damage in *K. pneumoniae*. HR-LCMS analysis putatively annotated 76 compounds, including alkaloids, saponins, and phenolic acids. Molecular docking revealed strong binding affinities of compounds such as 8′-Hydroxydihydroergotamine and Licoricesaponin E2 to CTX-M-15. The extract demonstrated moderate antioxidant activity and low cytotoxicity, with over 97% cell viability in fibroblast assays.

Conclusions: B. amyloliquefaciens NWR-14 shows promise as a source of bioactive secondary metabolites with antibacterial, antibiofilm, and antioxidant properties. These findings underscore the potential of endophytic bacteria from medicinal plants as reservoirs of compounds for addressing antimicrobial resistance. Further purification and structural validation of active constituents are recommended to enhance therapeutic applicability.

Introduction

The worldwide healthcare challenge posed by antibiotic resistance is intensified due to the declining efficacy of current antimicrobial therapies and the emergence of novel pathogens, including lethal viruses (Monowar et al., 2018). Contributing factors include poor hygiene

* Corresponding author at: School of Biosciences, Mar Athanasios College for Advanced Studies Tiruvalla, Pathanamthitta, Kerala, India.
E-mail address: smitha@macfast.org (S. Vijayan).

https://doi.org/10.1016/j.phyplu.2025.100885

Available online 20 September 2025

practices, antibiotic misuse, delayed diagnoses, and the vulnerability of immunocompromised individuals (Monowar et al., 2018). This growing resistance has fueled the urgent search for innovative antimicrobial agents. Natural substances derived from medicinal plants, fungi, and bacteria are increasingly recognized for their potential to combat drug-resistant pathogens due to their biocompatibility and abundance of bioactive compounds (Arifiyanto et al., 2023). These agents are particularly valuable because their interactions with microbial proteins reduce the likelihood of resistance development (Nisa et al., 2020). Recent studies have investigated these compounds as standalone therapies and in conjunction with antibiotics. (Arifiyanto et al., 2023).

Endophytes have emerged as a promising source of new antimicrobial compounds. These microorganisms inhabit healthy plant tissues without harming or causing disease and produce unique bioactive metabolites that can sometimes exceed the therapeutic effectiveness of host plants (Anh et al., 2022; Litao et al., 2023). Endophytes, including bacteria and fungi, are natural reservoirs of diverse bioactive compounds with significant pharmaceutical potential (Gouda et al., 2016). These metabolites include alkaloids, steroids, terpenoids, lactones, quinones, lignans, and phenols, many exhibiting potent antimicrobial properties (Anh et al., 2022). Although most plants harbour endophytic microbes, the endophytic communities of several plant species remain underexplored (Mengistu, 2020). This unexplored diversity holds immense potential for discovering novel therapeutic agents, particularly in combating antibiotic-resistant pathogens. Notably, researchers have identified bacterial endophytes from medicinal plants that produce metabolites comparable to or more effective than those synthesized by their host plants (Anh et al., 2022). These metabolites often mimic the bioactive compounds present in the host while providing increased activity, making them a valuable resource in meeting the global challenge of antibiotic resistance. In recent studies, isolated bacterial endophytes from medicinal plants have shown broad antimicrobial activity against drug-resistant pathogens (Mengistu, 2020; Sansinenea et al., 2020). The ability of endophytes to synthesize such diverse and potent compounds underscores their importance as a rich and largely untapped source of novel therapeutic agents.

Plants and their bacterial endophytes engage in a mutually beneficial relationship, where plants provide a protective habitat and nourishment for the endophytes, and the endophytes, in turn, shield the plants from herbivores and disease-causing pathogens through the production of bioactive compounds (Anh et al., 2022). Additionally, endophytic bacteria contribute to plant growth and resilience by synthesizing plant hormones such as auxins and gibberellins, enhancing plants' ability to tolerate environmental stressors, including high salinity and toxic heavy metals (Khan et al., 2014). The benefits of endophytic bacteria extend beyond their plant hosts, with significant applications in agriculture, industry, and medicine (Anh et al., 2022). For example, they can act as biocontrol agents to protect crops, produce industrial enzymes for biotechnological applications, and serve as sources of novel antimicrobial compounds for therapeutic use. Research focused on isolating bioactive compounds from bacterial endophytes holds great promise for discovering new molecules that can be developed into effective antimicrobial therapies, addressing the global challenge of antibiotic resistance.

Piper chaba W. Hunter, a member of the Piperaceae family, is a climbing vine predominantly found in India's tropical and subtropical regions. This vine spreads along the ground and climbs over large trees, featuring smooth, oval-shaped leaves measuring approximately 2 to 3 inches in length. It produces single-fruit flowers blooming during the rainy season, which increases its ecological adaptability. The long fruits of *P. chaba*, similar to other long pepper varieties, grow up to 3 inches. First, when mature, the fruit turns dark brown or black when dried (Islam et al., 2020). *P. chaba* has traditionally been used in ayurvedic practices for its medicinal properties, demonstrating its importance beyond its botanical characteristics.

Like other plants in the *Piper* genus, *P. chaba* holds significant folkloric and traditional medicinal value. The root is believed to possess alexiteric properties and is widely used in managing respiratory ailments such as asthma, bronchitis, and consumption. The fruit, known for its pungent and thermogenic characteristics, is also anthelmintic, expectorant, and carminative, enhancing appetite and alleviating ailments like asthma, bronchitis, fever, inflammation, piles, and abdominal discomfort. Additionally, the fruit is a stimulant that is effective in treating hemorrhoidal conditions. The stem is traditionally used to ease postpartum pain in mothers and has shown efficacy in managing rheumatic pain and diarrhoea (Islam et al., 2020). Due to its wide-ranging therapeutic applications, *P. chaba* was chosen for the study to explore bacterial endophytes, recognized for producing bioactive compounds. The research aimed to evaluate these endophytic strains for their antibacterial efficacy against ESBL producing *Klebsiella pneumoniae*, a major cause of hospital-acquired infections worldwide. This pathogen produces ESBL enzymes, conferring resistance to third-generation cephalosporins and monobactams, making treatment increasingly challenging. The United States Centers for Disease Control and Prevention (CDC), along with Public Health England and the World Health Organization (WHO), classify *K. pneumoniae* as a multidrug-resistant organism and an urgent global health threat. (Asokan et al., 2025).

Materials and methods

All chemicals and media used in this investigation, including antibiotics and nutrient agar, were supplied by Hi-Media Laboratories, Mumbai, India**.** The Clinical Microbiology Laboratory at Pushpagiri Medical College Hospital, a 900-bed tertiary care facility in Tiruvalla, Kerala, India, provided the clinical strains of *K. pneumoniae* that produce extended-spectrum beta-lactamases (ESBLs). Clinical strains were anonymized to preserve patient privacy. The Pushpagiri Institute of Medical Sciences & Research Centre's Institutional Review Board (IRB) gave the study ethical approval (Approval No: IRB/03/10/2023).

In compliance with the 2023 Clinical and Laboratory Standards Institute (CLSI) M100 guidelines, the disk diffusion method was used to detect ESBL production phenotypically. Antibiotic discs were used for antibiotic susceptibility testing, and CLSI criteria were used to measure and interpret the zone of inhibition. For short-term storage, bacterial cultures were kept on nutrient agar slants at 4 °C. They were then routinely subcultured to ensure their viability for upcoming studies.

Collection of plant

P. chaba was collected from the Pharmacognosy Unit of the Regional Ayurveda Research Institute (RARI), Poojappura, in Trivandrum District, Kerala. The Principal Scientist Dr. G. Rajkumar at JNTBGRI, Palode, Trivandrum, Kerala, identified the plant. The specimen was verified and included in their herbarium collection under the accession number 101,613.

Isolation of bacterial endophytes

Endophytic bacteria were extracted from healthy plant tissues after surface sterilization. After being cleaned with running tap water, the plant samples were left to air dry. Following desiccation, the various plant components (root, stem, leaf, and fruit) were sectioned into smaller pieces. The plant segments were subjected to a sequential surface sterilization protocol comprising an initial one-min treatment with 70 % ethanol, a five-min submersion in 5 % sodium hypochlorite (NaOCl), and a concluding 30 s rinse with 70 % ethanol. As the final step, the segments underwent a series of three rinses with sterile distilled water before being placed on sterile blotting paper to dry (Fig. 1).

The surface-sterilized plant segments were inoculated onto Nutrient Agar medium (composition: peptone 5 g/L, beef extract 3 g/L, NaCl 5 g/L, agar 15 g/L, pH 7.0) supplemented with the antifungal agent carbendazim (100 μg/mL) to suppress fungal mycelial growth and

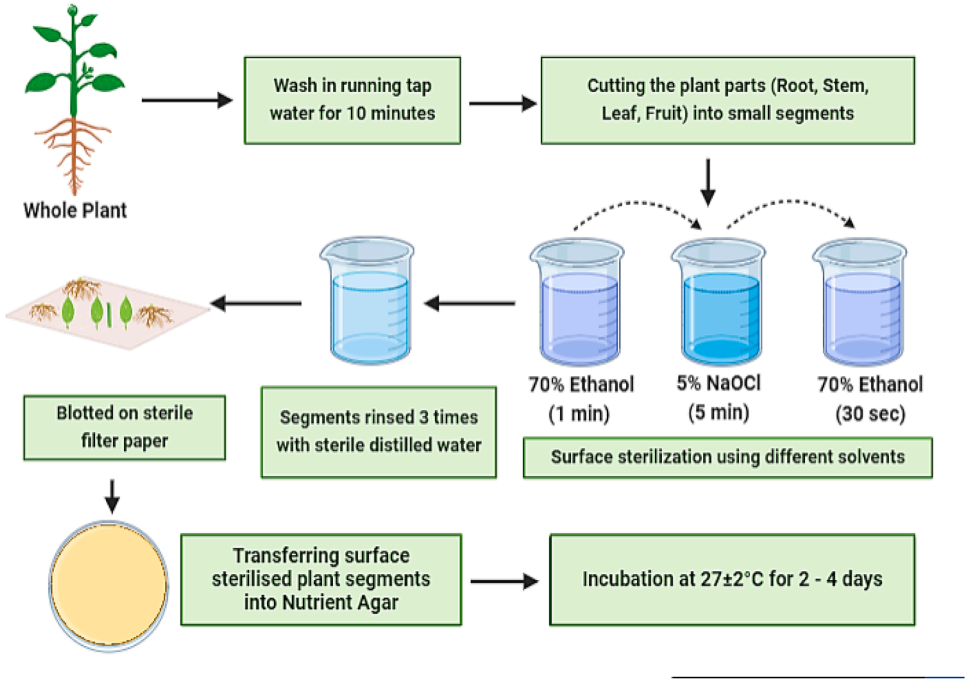

Fig. 1. Schematic representation of the surface sterilization procedure for plant segments.

selectively recover endophytic bacteria. To verify the adequacy of the sterilization process, the last wash with sterile distilled water was plated onto Nutrient Agar. Emerging colonies were transferred to fresh Nutrient Agar plates for further purification. Each purified colony was maintained as stock cultures on Nutrient Agar slants at 4 °C for subsequent use (Aswani et al., 2017).

Characterization of bacterial endophytes

The isolated endophytes were characterized by microscopic examination, and biochemical assays. Endophytic bacteria with antibacterial potential were identified by 16S rRNA sequencing.

Screening of bacterial endophytes for antibacterial activity

The agar well diffusion method and cross-streak assay were employed in this study.

Agar well diffusion method

Each endophytic isolate was cultured in 2 ml of sterile Mueller-Hinton broth in Eppendorf tubes. The cultures were incubated at 28 °C for 24 h with continuous shaking at a relative centrifugal force of approximately 200 × g**.** After incubation, the tubes underwent centrifugation to separate the supernatant from the cell pellet. The supernatant was then collected for further antimicrobial activity analysis. Mueller-Hinton agar plates were prepared with a lawn culture of *K. pneumoniae*, adjusted to match a 0.5 McFarland turbidity standard. Three wells were created in each plate using sterile micropipette tips: one for the bacterial sample, another for ceftazidime-avibactam (positive control), and a third for sterile distilled water (negative control). A 100 µl volume of the supernatant was added to the appropriate wells. Incubation at 37 °C was conducted for 24 h. Following incubation, the plates were examined for clear zones of inhibition surrounding the wells. These zones' diameters were measured to assess the antimicrobial efficacy of the supernatant (Aswani et al., 2017).

Cross streak assay

The antimicrobial properties of microorganisms were assessed using a qualitative approach known as the cross-streak assay (Aswani et al., 2017). This method involved the initial streaking of an endophytic bacterial isolate in a single, continuous line across an agar plate, followed by a period of growth. Subsequently, *K. pneumoniae* was streaked in an orthogonal direction, creating an intersection with the original isolate at the plate's midpoint. The interaction between the pathogen and the endophytic isolate was examined after a 24 h incubation period at 37 °C. Inhibition of the test pathogen's growth near the intersection was indicative of antimicrobial activity (Fig. 2).

Molecular characterization by 16S rRNA sequencing

To identify and characterize endophytic bacteria demonstrating strong antibacterial activity against ESBL producing *K. pneumoniae*, molecular characterization was carried out using 16S rRNA sequence analysis. DNA extraction followed the manufacturer's protocol using the NucleoSpin® tissue kit (Macherey-Nagel, Germany). The extracted DNA quality was evaluated using 1 % agarose gel electrophoresis, and the visualization was performed under ultraviolet light utilizing a gel documentation system.

The amplification of the 16S rRNA gene utilized the forward primer 5′-CAGGCCTAACACATGCAAGTC-3′ and the reverse primer 5′-GGGCGGWGTGTACAAGGC-3′ The PCR was conducted using a GeneAmp PCR System 9700 manufactured by Applied Biosystems (USA). The thermal cycling procedure started with an initial denaturation phase at 95 °C for 5 min. This was followed by 35 cycles. Each cycle consisted of three phases: first, denaturation at 95 °C for 30 s; next, annealing at 60 °C for 40 s; and finally, extension at 72 °C for 60 s. The reaction concluded with a final extension step at 72 °C for 7 min. After the synthesis, the PCR products were analyzed using 1.5 % agarose gel electrophoresis. The products were examined using ultraviolet light. A 100 bp DNA ladder served as a size reference.

Amplified PCR products are cleaned using ExoSAP-IT (USB, United States) to remove excess peptides and nucleotides. For sequencing, the BigDye Terminator v3.1 Cycle Sequencing Kit (Applied Biosystems,

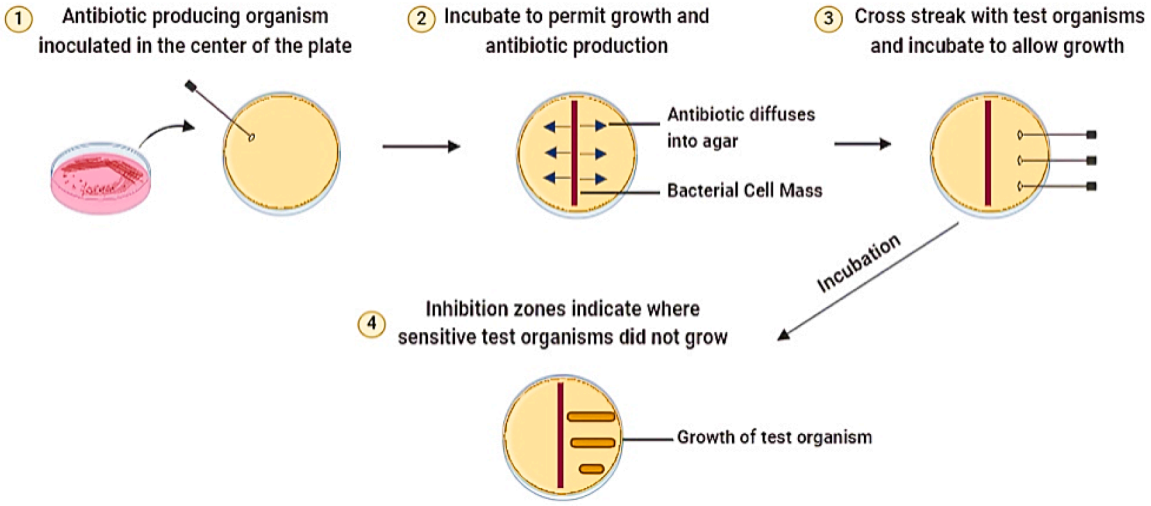

Fig. 2. Schematic diagram of the cross-streak assay for evaluating antimicrobial activity.

USA) was used. Sequence Scanner Software v1 (Applied Biosystems) analysed the resulting sequences for quality. The obtained sequences underwent homology analysis using NCBI-BLAST, comparing them to nucleotide sequences in the NCBI database. The isolate was identified based on the BLAST score and the degree of similarity between the 16S sequences. The sequence was later submitted to the NCBI GenBank database.

Characterization of virulence traits in isolated endophytic bacteria

The virulence potential of the isolated endophytic bacteria was assessed through two primary tests: the antibiotic sensitivity assay and the hemolysis test.

Antibiotic susceptibility assay

The antibiotic susceptibility of the endophytic bacteria was determined using the Kirby-Bauer disk diffusion method (Chen et al., 2019). The bacteria were incubated overnight in nutrient broth, and then a sterile cotton swab was employed to evenly distribute the culture over the surface of Mueller-Hinton Agar plates. Subsequently, antibiotic discs were placed on the surface of the agar, including Amikacin (30 μg), Gentamicin (10 μg), Ciprofloxacin (5 μg), Nalidixic Acid (30 μg), Levofloxacin (5 μg), Norfloxacin (10 μg), Tetracycline (30 μg), Erythromycin (15 μg), Penicillin (10 μg), Ampicillin (10 μg), Chloramphenicol (30 μg), Imipenem (10 μg), Colistin (10 μg), and Bacitracin (0.04 units). Based on the measured diameters of the inhibition zones for each antibiotic, expressed in millimetres, the bacteria were categorized as sensitive, intermediate, or resistant (Dabire et al., 2022). The following formula was used to determine the pathogen's Multiple Antibiotic Resistance Percentage (MAR %):

$$MAR\ \% = \frac{No\ of\ antibiotics\ to\ which\ the\ isolate\ showed\ resistance}{Total\ number\ of\ antibiotics\ tested} \times 100$$

Hemolysis test

To evaluate the hemolytic activity of endophytic bacterial isolates, the cultures were grown on blood agar plates and maintained at 37 °C for a duration of 24 to 48 h. This assessment aimed to determine how potentially harmful these isolates could be to humans and animals. A clear, distinct zone surrounding bacterial colonies on Blood Agar was a sign of hemolytic activity and could pose a risk to the health of both humans and animals. On the other hand, the lack of a clear zone around the colonies indicated no hemolytic activity, suggesting that these isolates might be safe for use (Dabire et al., 2022).

Preparation of extract for antibiosis studies

Endophytic bacteria were cultured in 100 ml of tryptic soy broth in four Erlenmeyer flasks and incubated with continuous shaking at approximately 120 × g for three days. Following incubation, bacterial cultures were combined with equal volumes of various solvents, including ethyl acetate, hexane, chloroform, and butanol. The mixture was continuously agitated and allowed to fractionate overnight. Filtration was performed using Whatman No. 1 filter paper, and the resultant filtrate was dried at 55 °C to obtain a crude extract (Chen et al., 2019). This dried extract was subsequently dissolved in 100 μl of 0.1 % DMSO and assessed for its antimicrobial activity against ESBL-producing *K. pneumoniae* using the agar well diffusion method (Fig. 3).

Determination of MIC and MBC

The lowest concentration of bacterial extracts that can inhibit bacterial growth is known as the minimum inhibitory concentration (MIC). It was determined using a microtitre plate-based antimicrobial assay with the resazurin method (Mekky et al., 2021). 100 μl of Mueller-Hinton broth was added to each well in columns 1 to 12 of the microtitre plate. Then, 100 μl of the bacterial extract (25 μg/ml) was added to the first well of column 1, followed by serial dilution across the plate up to column 10. Column 1 contained the highest concentration of the extract, while column 10 contained the lowest. Column 11 was the negative control (medium only), and column 12 was the positive control (medium with bacterial inoculum).

A total of 20 μl of *K. pneumoniae* suspension (1×10^8 CFU/ml) was added to each well, except for column 11 and incubated at 37 °C for 24 h. Following incubation, 50 μl of resazurin dye was added to each well, and the plate was reincubated for 4 h to assess bacterial viability. A lack of colour change in the resazurin (remaining blue or purple) indicated inhibition of bacterial growth by the crude extract. In contrast, a colour change to pink signified the presence of viable bacterial cells due to the oxidation of the dye. The MIC value refers to the minimum concentration of the crude extract that prevents observable bacterial growth.

The culture samples from each well were transferred onto Mueller-Hinton agar plates to determine the minimum bactericidal concentration (MBC). After that, these plates were incubated at 37 °C for 24 h. The MBC was identified as the lowest extract concentration that prevented

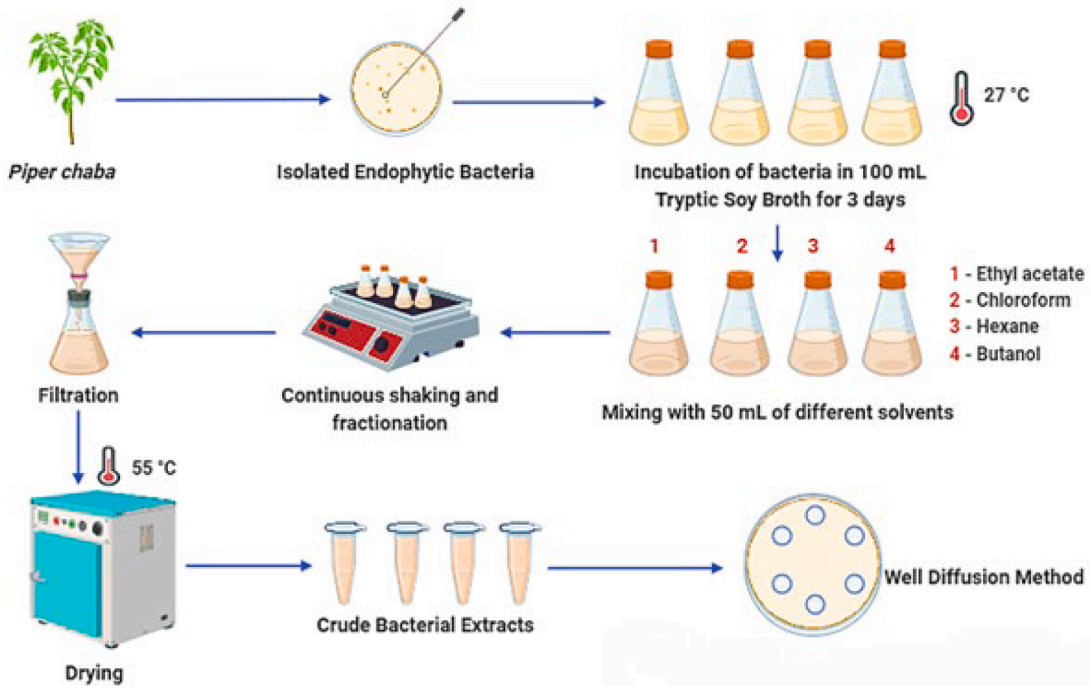

Fig. 3. Schematic overview of extraction and antibacterial screening of metabolites from endophytic bacteria.

visible bacterial growth on the agar's surface (Mekky et al., 2021).

Antibiofilm assay by test tube method

Five different concentrations of the endophytic bacterial extract (0.375 mg/ml, 0.75 mg/ml, 1.5 mg/ml, 3 mg/ml, and 6 mg/ml) were prepared for the experimental setup. In each test tube, 3 mL of sterile nutrient broth was combined with 3 ml of a standardized *K. pneumoniae* suspension (0.5 McFarland standard). To each tube, 0.5 ml of the designated concentration of the bacterial extract was added. Positive controls included 0.5 ml of 0.1 % DMSO, which served as a solvent for the extract and allowed uninhibited biofilm formation. Negative controls contained sterile nutrient broth without the bacterial culture or extract. The test tubes were maintained at a temperature of 37 °C for a duration of 72 h, during which they were agitated constantly to enhance the growth of biofilms on the surfaces within the tubes. Following

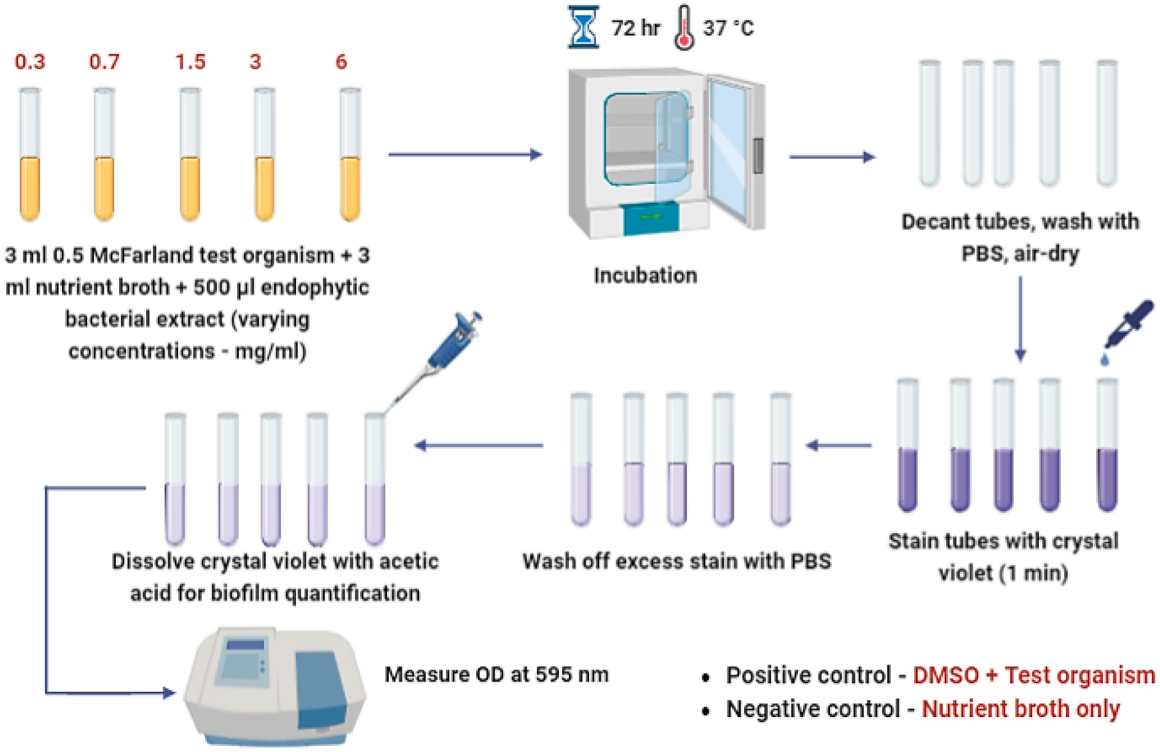

Fig. 4. Schematic illustration of the antibiofilm activity assay of endophytic bacterial extract against *K. pneumoniae*.

incubation, the liquid contents were discarded, and the tubes were gently rinsed with phosphate-buffered saline (PBS) to remove non-adherent cells. The tubes were air-dried to prepare them for subsequent biofilm analysis. To observe the biofilm, the tubes were dried and then subjected to staining with 0.1 % crystal violet for one min. Afterwards, excess dye was washed off with PBS, and the remaining stain was dissolved using 1 % acetic acid. Using a spectrophotometer, the absorbance at 595 nm was recorded to quantify the biofilm formation after staining with crystal violet (Fig. 4). A decrease in OD relative to the positive control was indicative of antibiofilm activity of the endophytic bacterial extract against *K. pneumoniae* (Chen et al., 2019).

Scanning electron microscopy analysis

The antibacterial mechanism of the endophytic bacterial extract was evaluated by observing morphological changes in K. pneumoniae using scanning electron microscopy (SEM). A fresh culture of K. pneumoniae was grown in sterile Mueller-Hinton broth (MHB) and adjusted to match the 0.5 McFarland standard. To 100 mL of this culture, 2 mL of the crude bacterial extract (1.56 mg/mL) was added, followed by incubation at 37 °C for 12 h under shaking conditions. A control sample without extract treatment was processed in parallel (Vijayan et al., 2020).

After incubation, samples were centrifuged at 10,000 × g for 10 min (Vijayan et al., 2020), and the resulting pellets were resuspended in sterile Milli-Q water. A 10 µL aliquot of each suspension was placed on a sterile glass slide and air-dried. Prior to imaging, samples were sputter-coated with a thin layer of gold to improve conductivity and image resolution. SEM analysis was performed using a JEOL JSM-6390 scanning electron microscope equipped with a tungsten filament electron source and capable of achieving a resolution of approximately 3 nm. Imaging was conducted using secondary electron (SE) and backscattered electron (BSE) modes under high vacuum. Accelerating voltages between 5 and 15 kV were applied, and images were acquired at magnifications ranging from 1000 × to 50,000 × to observe ultrastructural alterations in bacterial cells. The system includes auto-focus and auto-stigmation features to optimize image quality.

Annotation of bioactive compounds by HR-LCMS analysis

The crude extract was subjected to high-resolution liquid chromatography mass spectrometry (HR-LCMS) for secondary metabolite profiling. The analysis was performed at the Sophisticated Analytical Instrument Facility (SAIF), Indian Institute of Technology (IIT) Bombay, using an Agilent 1290 Infinity UHPLC system coupled with an Agilent 6550 iFunnel QTOF HR-LCMS. This Orbitrap-type high-resolution system operates across a mass range of m/z 50–3200 with a mass accuracy typically within 1 ppm and a resolution of 40,000 full width at half maximum (FWHM). The instrument demonstrated high sensitivity, achieving a signal-to-noise ratio of 100:1 for 1 pg of reserpine. Chromatographic separation was achieved on an Agilent Eclipse Plus C18 reversed-phase column (2.1 × 100 mm, 1.8 µm particle size). The mobile phases consisted of solvent A (water with 0.1 % formic acid) and solvent B (acetonitrile with 0.1 % formic acid). A linear gradient from 5 % B to 95 % B was applied over 25 min, followed by re-equilibration, with a total runtime of 30 min. The flow rate was maintained at 0.3 mL/min, and the column oven temperature was set to 30 °C. Mass spectrometric analysis was carried out using both electrospray ionization (ESI) and atmospheric pressure chemical ionization (APCI) in positive and negative ionization modes. Direct infusion was used to acquire data in both MS and MS/MS modes. Ionization parameters included an ion spray voltage of −3.5 kV and a capillary temperature of 320 °C.

Molecular docking studies of the annotated compounds

A total of 76 compounds annotated through HR-LCMS profiling were retrieved from the PubChem database for molecular docking analysis to assess their potential antibacterial activity. The *K. pneumoniae* CTX-M-15 enzyme (PDB ID: 5T66), a well-characterised ESBL, was selected as the target protein for this study. CTX-M-15 plays a crucial role in β-lactam antibiotic resistance by hydrolyzing penicillins and cephalosporins. Inhibiting CTX-M-15 has been shown to restore the efficacy of β-lactam antibiotics more effectively than efflux pump inhibition, which only indirectly reduces resistance (Bush, 2018; Jamil et al., 2023).

The three-dimensional (3D) structure of CTX-M-15 was retrieved from the RCSB Protein Data Bank (https://www.rcsb.org) and pre-processed using BIOVIA Discovery Studio Visualizer. The preparation step involved the removal of water molecules and co-crystallized ligands to ensure a clean protein structure for docking studies. Molecular docking simulations were performed using AutoDock Vina 4.2 to predict the binding affinities and interactions between the test compounds and CTX-M-15. A grid box was defined around the active site of the protein to optimize ligand-protein interactions (Degfie et al., 2022).

Post-docking analyses were conducted using PyMOL and BIOVIA Discovery Studio Visualizer to evaluate the binding interactions, including hydrogen bonding, hydrophobic interactions, and other molecular forces at the active site. These interactions were analyzed to determine the potential inhibitory effects of the selected compounds against CTX-M-15 (Degfie et al., 2022).

Antioxidant activity

DPPH assay

The antioxidant activity of raw bacterial extracts was assessed using a modified procedure based on Degfie et al. (2022). A 1 ml aliquot of DPPH solution (0.1 mM in methanol) was combined with 1 ml of the crude extract at different concentrations. The mixture was kept in the dark for 30 min at room temperature, and absorbance was measured at 517 nm using a spectrophotometer. Methanol served as the blank, and the DPPH solution without the crude extract acted as the control. Ascorbic acid served as the reference standard. A reduction in absorbance indicated the sample's capacity to neutralize free radicals. To evaluate the DPPH radical scavenging activity, the following equation was employed:

$$DPPH\ Scavenging\ activity\ (\%) = \frac{(Acontrol - Asample)}{Acontrol} \times 100$$

FRAP assay

Different concentrations of the sample (500 µl) were combined with 1.5 ml of 0.2 M sodium phosphate buffer (pH 6.6) and 1.5 ml of 1 % potassium ferricyanide solution. This mixture was incubated at 50 °C for 20 min. Following incubation, 5 ml of 10 % trichloroacetic acid was added, and the solution was centrifuged at an estimated 6000 × g for 5 min at 4 °C. From the resulting supernatant, 1.5 ml was collected and mixed with 1.5 ml of distilled water and 300 µl of 0.1 % ferric chloride solution. The absorbance of the final solution was measured at 700 nm, with ascorbic acid used as a reference standard. A higher absorbance indicated a greater reducing power of the sample. The concentration that corresponded to an absorbance of 0.5 was used as the benchmark to determine the reducing potential of each sample (Arifiyanto et al., 2023).

ABTS assay

The antioxidant activity of the sample extract was evaluated using the ABTS radical scavenging assay, which is based on electron transfer. In this method, antioxidants help convert the dark blue ABTS radical cation, formed from 2,2′-azino-bis(3-ethylbenzothiazoline-6-sulfonate), into a colorless ABTS molecule (Arifiyanto et al., 2023). The reaction was initiated by mixing 200 µl of diluted ABTS solution with varying volumes of the sample extract (31.25, 62.5, 125, 250, and 500 µl). As a

control, 50 µl of methanol was used in place of the sample extract, and the blank was also prepared with methanol. At 734 nm, absorbance values were measured, and the radical inhibition percentage was determined using the equation provided below:

$$Percentage\ inhibition = \frac{(Acontrol - Asample)}{Acontrol} \times 100$$

Cytotoxic activity (MTT assay)

To evaluate the metabolic activity of microorganisms, reflecting cell viability, growth, and cytotoxic effects, the MTT assay was employed (Mosmann et al., 1983). The National Center for Cell Sciences (NCCS), located in Pune, India, provided the L929 mouse fibroblast cell line utilized in this investigation. A 96-well plate was seeded with 10,000 cells per well, and the cells were left to acclimate for 24 h at 37 °C in an environment with 5 % CO_2. The chemical of interest was dissolved in 100 µL/ml of Dulbecco's Modified Eagle Medium (DMEM) to prepare the test sample and then sterilized using a 0.2 µm Millipore syringe filter. Substances were introduced to the grown cells in 20, 40, 60, 80, and 100 µl increments, while control wells were left untreated. All experiments were carried out in triplicate to reduce variability and guarantee reproducibility.

The plates were incubated for a full day after adding the test samples. After discarding the medium, each well received 100 µl of MTT solution (0.5 mg/ml in phosphate-buffered saline or PBS). The supernatant was carefully removed after a 2-hour incubation to promote the development of formazan crystals, and 100 µl of 100 % dimethyl sulfoxide (DMSO) was added to dissolve the formazan crystals. A microplate reader was used to measure the OD at 570 nm. Three cell-free wells served as blanks to create baseline readings. Three duplicates of each experiment were carried out, and the mean values were analyzed. The following formula was used to estimate cell viability:

$$Percentage\ ofcell\ viability = \frac{Average\ absorbance\ oftreated}{Average\ absorbance\ of\ control} \times 100$$

Statistical analysis

To ensure the accuracy and consistency of the findings, every test was conducted three times. The findings are presented as mean values ± standard deviation (SD), highlighting the dependability and variability of the data.

Results

Isolation and characterization of endophytic bacteria with antibacterial activity

To examine the occurrence of endophytic bacteria, a comprehensive analysis was conducted on 40 sections of *P. chaba*, including 3 root sections, 12 stem sections, 16 fruit sections, and 9 leaf sections from various plants. The bacterial isolates were assigned alphanumeric codes corresponding to the plant part they originated from: leaves (PLL), roots (PLR), stems (PLS), and fruits (PLF) (Fig. 5). After surface sterilization, a total of 40 bacterial isolates were obtained from the root, stem, fruit, and leaf samples (Fig. 6). The effectiveness of the sterilization process was confirmed by the absence of microbial growth on control plates after a three-day incubation period at room temperature.

The cultural and morphological characteristics of the bacterial isolates were meticulously examined. The findings were systematically documented and presented in Supplementary Table S2. Gram staining analysis was conducted on the isolates, revealing that 39 out of 40 were Gram-positive, while a single isolate was Gram-negative.

Among the various endophytic bacteria isolated, strain PLS06, derived from the stem, exhibited remarkable antibacterial activity against ESBL-producing *K. pneumoniae*. This was demonstrated through the agar well diffusion method (Fig. 7a and Table 1) and the cross-streak assay (Fig. 7b and Table 2), with the former yielding a 20 mm zone of inhibition.

The PLS06 isolate was subjected to 16S rRNA gene sequencing at the Regional Facility for DNA Fingerprinting (RFDF), Rajiv Gandhi Centre for Biotechnology (RGCB), Trivandrum, Kerala. The obtained sequence was analyzed using the Basic Local Alignment Search Tool (BLAST) in the National Center for Biotechnology Information (NCBI) database. The homology analysis revealed a 100 % similarity with *Bacillus amyloliquefaciens* strain NWR-14, confirming its identity. The sequence data has been deposited in GenBank, and it has been assigned the accession number PP976621. A phylogenetic tree supporting the taxonomic identification has also been created and is included as Supplementary Fig. S5.

Antibiotic susceptibility assay

The antibiotic susceptibility profile of the endophytic bacterium *B. amyloliquefaciens* NWR-14 was evaluated against 14 antibiotics through the disk diffusion method (Fig. 8). The analysis shows that tetracycline, erythromycin, penicillin, ampicillin, colistin, and bacitracin were resistant to *B. amyloliquefaciens* NWR-14. At the same time, the isolate demonstrated sensitivity towards amikacin, gentamicin, ciprofloxacin, nalidixic acid, levofloxacin, norfloxacin, chloramphenicol, and imipenem. The Multiple Antibiotic Resistance (MAR) index was determined to be 42 %, suggesting that the isolate had only limited or moderate exposure to commonly used antibiotics and chemotherapeutic agents, thereby confirming its classification as a natural isolate. The antibiotic sensitivity patterns of the *B. amyloliquefaciens* NWR-14 expressed as zone of inhibition (mm), are presented in Table 3.

Hemolysis test

B. amyloliquefaciens NWR-14 cultured on blood agar medium for 24 to 48 h exhibited no hemolytic activity, as evidenced by the absence of a clear zone surrounding the bacterial colonies (Fig. 9a and b). The lack of hemolytic activity suggests that these isolates are safe for use in humans and animals, as they do not pose a risk of pathogenicity.

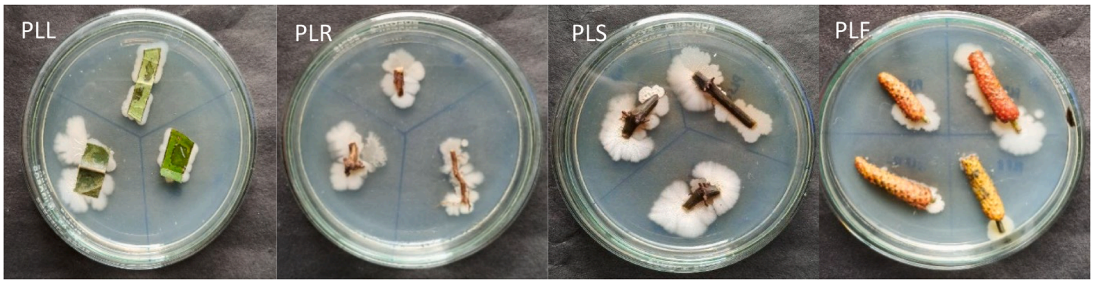

Fig. 5. Endophytes grown on surface-sterilized explants after 2–3 days of incubation on nutrient agar.

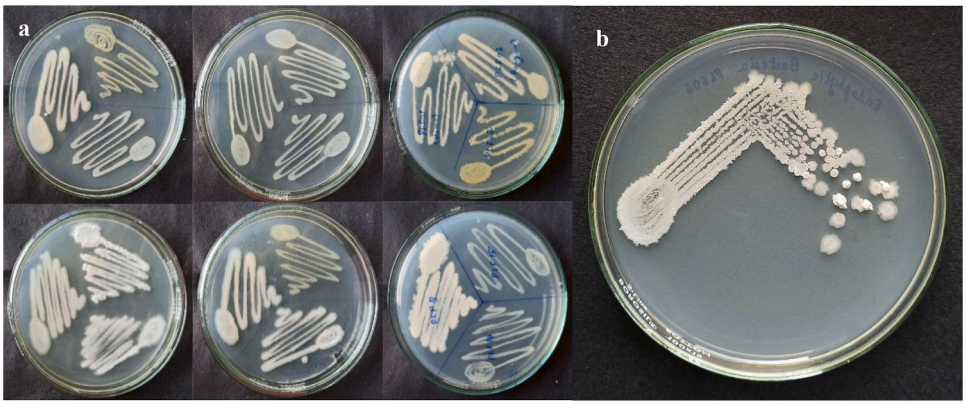

Fig. 6. (**a**) Endophytic bacterial isolates from P. chaba and (**b**) colony characteristics of Bacillus amyloliquefaciens NWR-14.

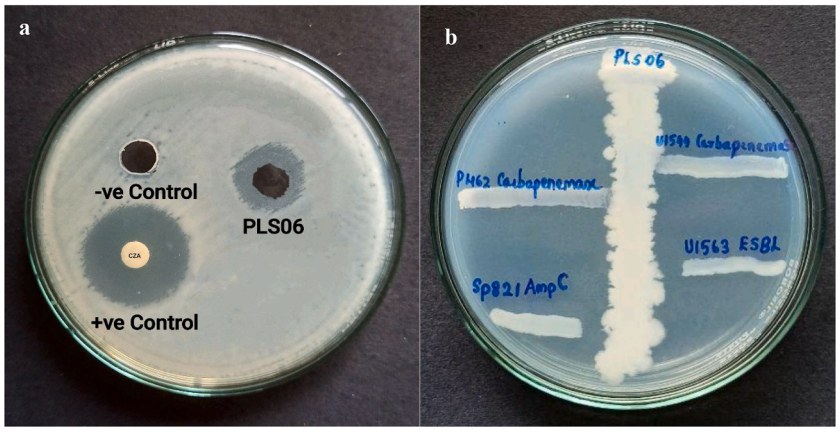

Fig. 7. Antibacterial activity of PLS06 by (**a**)Agar well diffusion method and (**b**) Cross streak assay showing inhibition of different β-lactamase-producing *K. pneumoniae*strains: ESBL (U1563), AmpC (SP821), and Carbapenemase producers (P462, U1544).

Table 1
Antibacterial activity of PLS06 by Agar well diffusion method.

Test Organism	Zone of inhibition (in mm)		
	PLS06	Ceftazidime-avibactam (+ve)	Distilled water (-ve)
ESBL *K. pneumoniae*	20 ± 0.1	25 ± 0.0	Nil

Table 2
Antibacterial activity of PLS06 against four *K. pneumoniae* strains via Cross streak assay.

Test Isolate	Zone of Inhibition (in mm)
U1563 ESBL	5 5 ± 0.0
SP821 AmpC	5 ± 0.0
P462 Carbapenemase	Nil
U1544 Carbapenemase	Nil

Antibacterial activity of the crude extract by well diffusion assay

The bioactive compounds from *B. amyloliquefaciens* were extracted using equal volumes of various solvents, including ethyl acetate, hexane, chloroform, and butanol. Each solvent fraction was filtered, evaporated to dryness, and reconstituted in 0.1 % DMSO for further evaluation. Antibacterial activity was assessed against ESBL producing *K. pneumoniae* using the agar well diffusion assay (Fig. 10). The ethyl acetate and butanol fractions exhibited the strongest antibacterial activity, while the hexane and chloroform fractions demonstrated comparatively weaker activity (Table 4).

Determination of MIC and MBC

The MIC of the ethyl acetate extract from *B. amyloliquefaciens* against *K. pneumoniae* was 1.56 mg/ml, as assessed through a resazurin-based microtiter plate assay. The absence of a colour change in the resazurin dye (remaining blue or purple) at this concentration indicated inhibition of bacterial growth (Fig. 11). Additionally, after a 24 h incubation period at this concentration, the extract showed no bacterial growth on Mueller Hinton agar plates, indicating a MBC of 1.56 mg/ml. Since the ethyl acetate extract inhibits bacterial growth and kills the bacteria at the same concentration, the identical MIC and MBC values imply that the extract has potent bactericidal effects.

Antibiofilm assay

To evaluate the inhibitory effect of the ethyl acetate extract from *B. amyloliquefaciens* on *K. pneumoniae* biofilms, the optical density (OD) of dissolved crystal violet was measured at 595 nm. To assess the extract's ability to inhibit biofilm formation, OD measurements taken at various extract concentrations were contrasted with the positive control (OD = 0.7936), as illustrated in Fig. 12a.

The experimental findings demonstrated a concentration-dependent reduction in biofilm formation as the concentration of the bacterial extract increased. At 0.375 mg/ml, the OD reading of 0.616 indicated a slight inhibition in biofilm development compared to the positive control. Additional decreases in biofilm formation were observed with OD

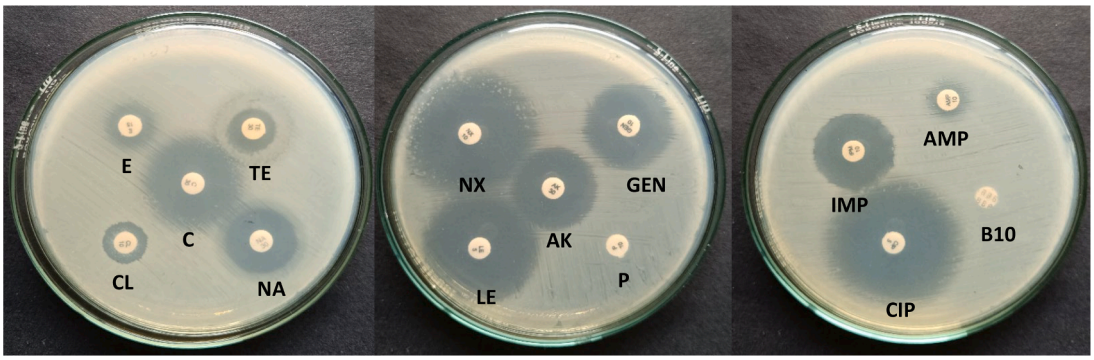

Fig. 8. Antibiotic sensitivity pattern of Bacillus amyloliquefaciens NWR-14 determined by the Kirby-Bauer disk diffusion method.

Table 3
Antibiotic susceptibility pattern of *B. amyloliquefaciens* NWR-14.

Antibiotic class	Antibiotic	Disc potency (μg)	Diameter of inhibition zone (mm)
Aminoglycosides	Amikacin (AK)	30	23 ± 0.0
	Gentamicin (GEN)	10	25 ± 0.0
Fluoroquinolones	Ciprofloxacin (CIP)	5	37 ± 0.0
	Nalidixic acid (NA)	30	20 ± 0.0
	Levofloxacin (LE)	5	33 ± 0.0
	Norfloxacin (NX)	10	37 ± 0.0
Tetracyclines	Tetracycline (TE)	30	13 ± 0.0
Macrolide	Erythromycin (E)	15	12 ± 0.0
	Penicillin (P)	10	Nil
Penicillin	Ampicillin (AMP)	10	12 ± 0.0
Phenicol	Chloramphenicol	30	26 ± 0.0
β-lactam Carbapenems	Imipenem (IMP)	10	23 ± 0.0
Lipopeptide	Colistin (CL)	10	12 ± 0.0
Cyclic Polypeptide	Bacitracin (B10)	0.04 units	Nil

values of 0.531 and 0.523 for concentration increases to 0.75 mg/ml and 1.5 mg/ml, respectively. The strongest antibiofilm activity was seen at higher concentrations; OD values of 0.304 and 0.252 were obtained for 3 mg/ml and 6 mg/ml, respectively (Fig. 12b). These concentrations exhibited the most pronounced inhibitory effect on biofilm formation, as evidenced by the substantial reduction in OD relative to the control. With the highest levels of inhibition occurring at the 3 mg/ml and 6 mg/ml concentrations, the data clearly show that the bacterial extract has concentration-dependent antibiofilm activity against *K. pneumoniae.*

SEM analysis

The SEM analysis revealed the irreversible damage inflicted on bacterial cells by the ethyl acetate extract of *B. amyloliquefaciens. K. pneumoniae* appears as rod-shaped structures, and smooth surfaces indicate intact bacterial cells (Fig. 13a). The attachment of the extract to the bacterial cells and its presence inside the cells serve as key evidence supporting the proposed mechanism of action (Fig. 13b).

Annotation of bioactive compounds by HR-LCMS analysis

Using HR-LCMS, the secondary metabolites of *B. amyloliquefaciens* were thoroughly examined, revealing a diverse array of putatively annotated bioactive compounds. A total of 76 metabolites were tentatively assigned based on accurate mass measurements, with retention times ranging from 1.499 to 24.912 min. Annotations were performed in both positive and negative electrospray ionization (ESI) modes. These compounds were classified into several chemical categories, including organosulfur compounds, amino acid derivatives, dipeptides, triterpenoids, alkaloids, phenolic acids, and saponins. The putatively annotated compounds are associated with known biological activities such as antibacterial, antioxidant, anti-inflammatory, antitumor, and neuroprotective effects (Table 5) as reported in existing literature. The chromatograms (Fig. 14a, b) displayed prominent peaks, indicating the presence of multiple metabolite candidates.

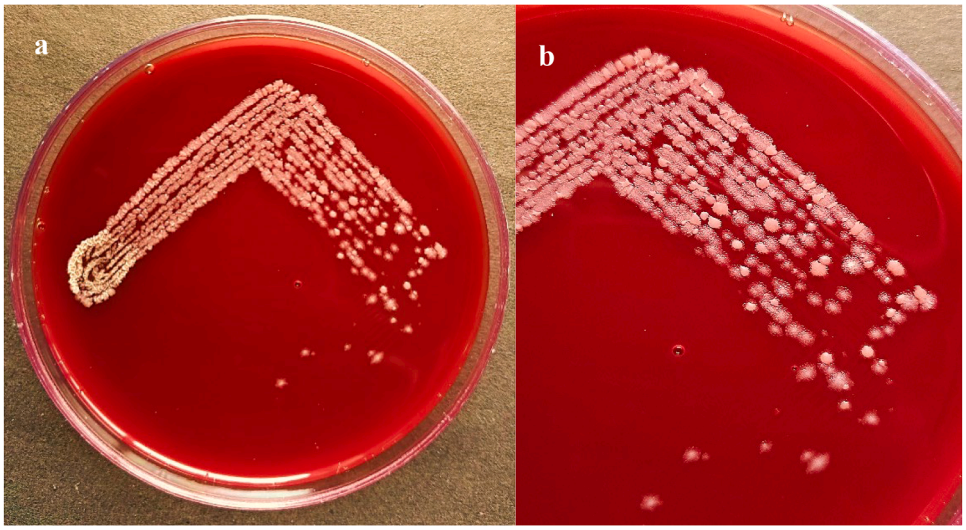

Fig. 9. Hemolytic activity test of (**a**) *B. amyloliquefaciens*on blood agar showing (**b**) the absence of a clear zone, indicating negative hemolysis.

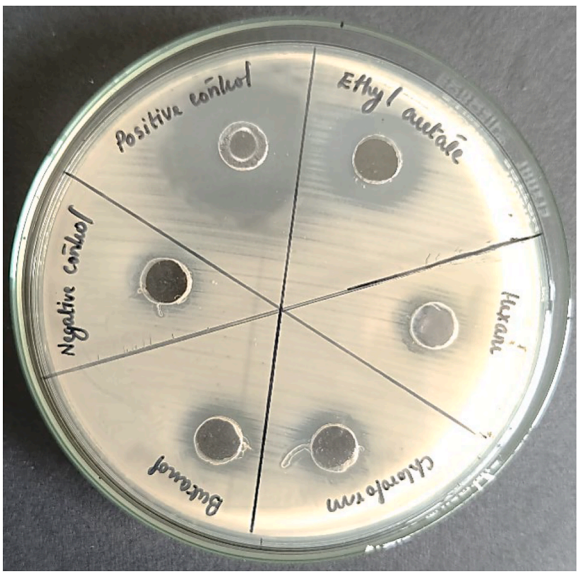

Fig. 10. Antibacterial activity of solvent extracts from *B. amyloliquefaciens.*

Table 4
Antibacterial activity of solvent-extracted fractions from *B. amyloliquefaciens* against ESBL-producing *K. pneumoniae.*

Extraction solvents	Agar Well Diffusion Assay (*K. pneumoniae*) Diameter of Inhibition Zone, mm
Ethyl acetate	12 ± 0.1
Hexane	10 ± 0.2
Chloroform	9 ± 0.1
Butanol	11 ± 0.1
Positive control (Ceftazidime-avibactum)	21 ± 0.0
Negative control (DMSO)	Nil

Among the putatively annotated compounds, 3-Methyl sulfolene (RT: 1.916, $C_5H_8O_2S$, ppm: 11.76) was notable for its reported antibacterial and antifungal properties. Similarly, (E)-Avenanthramide D (RT: 3.666, $C_{16}H_{13}NO_4$, ppm: –9.56) is associated with antioxidant, anti-inflammatory, and antitumor activities in the literature. The macrolide antibiotic Mycinamicin I (RT: 6.157, $C_{37}H_{61}NO_{12}$, ppm: –2.36) has been described as a potent antibacterial agent, while Momordicin II (RT: 8.964, $C_{36}H_{58}O_9$, ppm: 12.65), a triterpenoid saponin, has demonstrated both anticancer and anti-inflammatory effects.

In addition to these compounds, several putatively annotated bioactive peptides were detected. These included l-isoleucyl-l-proline (RT: 5.266, $C_{11}H_{20}N_2O_3$, ppm: 13.33), which is associated with antibacterial and antioxidant properties, and Tyrosyl-Leucine (RT: 6.094, $C_{15}H_{22}N_2O_4$, ppm: 14.33), known for its antimicrobial activity. Another compound, d-Tryptophan (RT: 5.389, $C_{11}H_{12}N_2O_2$, ppm: 13.66), was annotated as a serotonin precursor with reported antioxidant and antimicrobial potential.

The detection of these numerous bioactive metabolites highlights *B. amyloliquefaciens* as a prolific producer of pharmacologically significant compounds. These metabolites, due to their broad range of biological activities, have immense potential for therapeutic applications. Future research will focus on isolating individual compounds from the ethyl acetate fraction to evaluate their specific biological activities in detail, which will help in further understanding their potential use in drug development and other therapeutic areas.

Molecular docking studies of the annotated compounds

Molecular docking screening revealed that 28 of the 76 evaluated compounds exhibited notable binding affinities for the CTX-M-15 enzyme, with docking scores between −6.0 and −8.8 kcal/mol. The most promising interaction was observed with 8′-Hydroxydihydroergotamine (−8.8 kcal/mol), while Licoricesaponin E2 ranked second (−8.2 kcal/mol). Additional compounds, such as 11-Hydroxyyohimbine (−8.1 kcal/mol), Cholic acid glucuronide (−7.9 kcal/mol), and Momordicin II (−7.7 kcal/mol), also displayed substantial binding interactions with CTX-M-15.

The docking scores for all 28 active compounds are detailed in supplementary file. Furthermore, Fig. 15 provides 3D and 2D representations of the selected compounds exhibiting strong binding interactions within the enzyme's active site, emphasizing key residues involved in stabilization. These interactions include hydrogen bonds, hydrophobic contacts, and π-π stacking, which enhance complex stability. The high binding affinities suggest that these compounds could

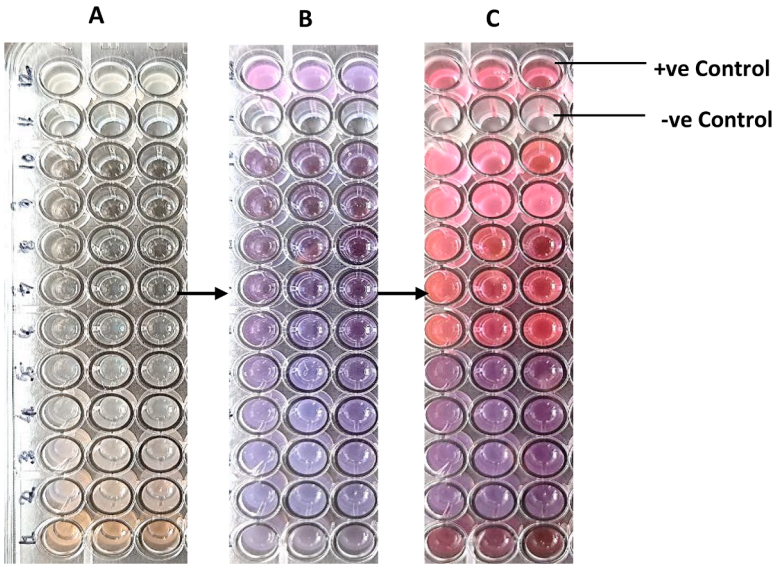

Fig. 11. MIC of the ethyl acetate extract of *B. amyloliquifaciens*by resazurin dye reduction method: (**A**) Cart preparation, (**B**) after the addition of resazurin dye, and (**C**) the results after incubation. A concentration of 1.56 mg/mL inhibited visible growth and showed no bacterial regrowth upon subculturing, indicating bactericidal activity. +ve Control: bacterial culture without extract; −ve Control: media only.

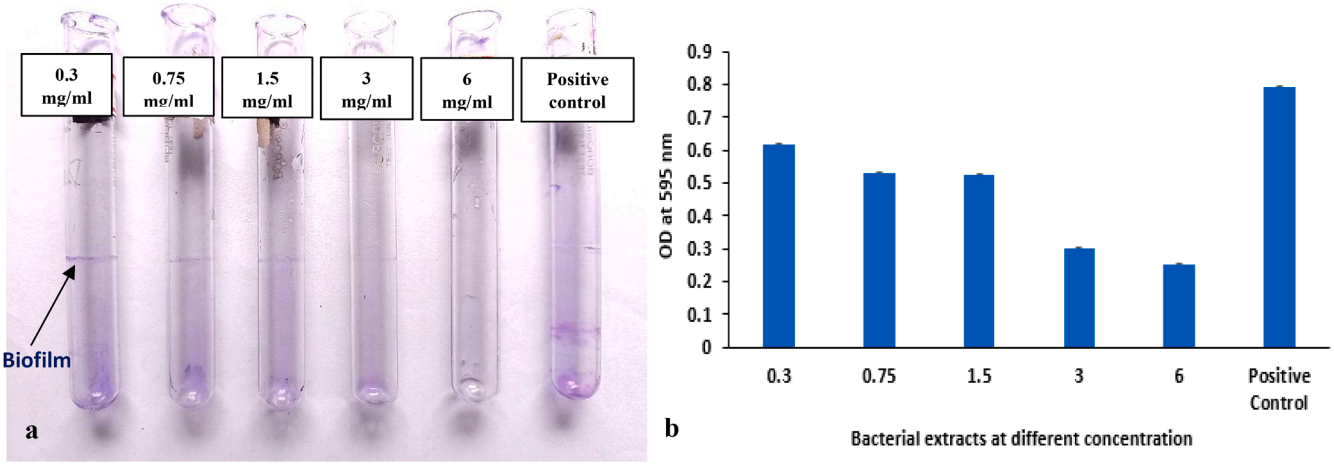

Fig. 12. Dose dependent Antibiofilm activity of bacterial extracts. (**a**) Bacterial biofilm developed on control and bacterial extract treated test tubes (**b**) Plot showing the variation in the biofilm developed on control and bacterial extract treated test tubes.

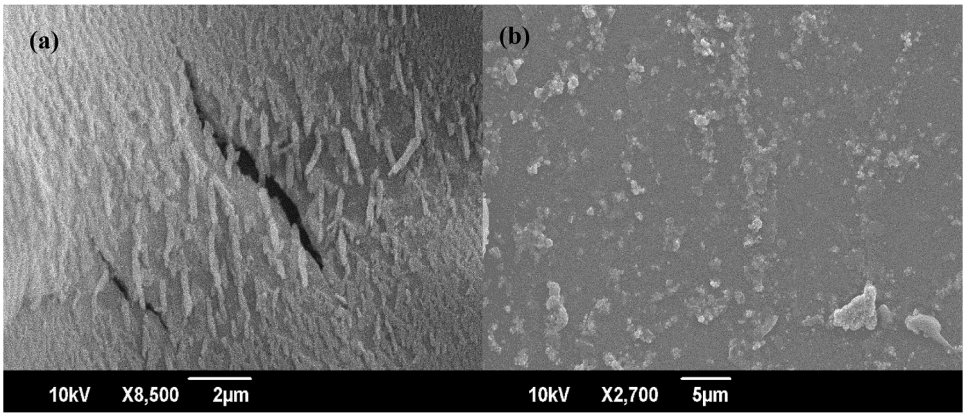

Fig. 13. SEM images of bacterial cells. (**a**) Samples of *K. pneumoniae* untreated and (**b**) treated with ethyl acetate extract (1.56 mg/mL) of *B. amyloliquifaciens* NWR-14.

act as potential CTX-M-15 inhibitors, offering a foundation for designing new therapeutic agents to combat β-lactam resistance in *K. pneumoniae.*

DPPH assay

The reducing capacity of the ethyl acetate extract from *B. amyloliquefaciens* was evaluated. The concentration corresponding to an absorbance of 0.5 was used as the benchmark for assessing the reducing potential of the samples. Ascorbic acid, used as a positive control, exhibited a concentration of 37.379 µg/ml at an absorbance of 0.5. On the other hand, the ethyl acetate extract of *B. amyloliquefaciens* had a much lower reducing power than ascorbic acid, requiring a concentration of 365.428 µg/ml to achieve the same absorbance. The IC50 value, indicating the concentration of the sample needed to scavenge 50 % of free radicals, was calculated as 170.795 µg/ml for the ethyl acetate extract of *B. amyloliquefaciens*. In contrast, the IC50 value of the reference standard, ascorbic acid, was notably lower at 10.462 µg/ml, demonstrating its significantly stronger antioxidant activity compared to the bacterial extract (Table 6). The findings indicate that although the ethyl acetate extract of *B. amyloliquefaciens* exhibits antioxidant potential, its scavenging activity is weaker than that of ascorbic acid.

FRAP assay

The reducing capacity of *B. amyloliquefaciens* ethyl acetate extract was assessed. The standard for evaluating the sample's reducing potential was the concentration corresponding to an absorbance 0.5. As a positive control, ascorbic acid showed an absorbance of 0.5 and a 37.379 µg/ml concentration. On the other hand, the ethyl acetate extract of *B. amyloliquefaciens* had a significantly lower reducing power than ascorbic acid, requiring a higher concentration of 365.428 µg/ml to achieve the same absorbance (Table 6).

ABTS assay

The antioxidant properties of the ethyl acetate extract derived from *B. amyloliquefaciens* were assessed through the ABTS radical scavenging assay (Table 6). The inhibition rates were determined across different extract concentrations by recording the absorbance at 734 nm. The standard was ascorbic acid, and the blank was methanol. The ABTS radical scavenging activity of the ethyl acetate extract was concentration dependent. The percentage inhibition increased progressively from 21.98 % to 68.15 % at concentrations ranging from 31.25 µl to 500 µl. The IC50 value of the extract was calculated to be 200.34 µl, derived from the slope equation obtained through linear regression analysis of the inhibition percentages versus the tested concentrations. On the other hand, the standard antioxidant ascorbic acid demonstrated superior radical scavenging activity with an IC50 value of 15.99 µg/ml. These results highlight the antioxidant capacity of *B. amyloliquefaciens* ethyl acetate extract, demonstrating significant scavenging activity at elevated concentrations.

Table 5
Bioactive Compounds Annotated in *B. amyloliquefaciens* through HR-LCMS Analysis: ESI Positive (1–22) and Negative (23–76) Modes.

Sl. No.	Identified Compound Name	Class of Compounds	RT (min)	Formula	ppm
1	3-methyl sulfolene	Organosulfur	1.916	$C_5H_8O_2S$	11.76
2.	L-methionine	Essential amino acid	2.026	$C_5H_{11}NO_2S$	8.33
3.	(Z)-2-hexenal	Unsaturated aldehyde	2.702	$C_6H_{10}O$	−8.86
4.	L-trans-5-Hydroxy-2- piperidinecarboxylic acid	Hydroxylated amino acid derivative	1.81	$C_6H_{11}NO_3$	3.015
5.	(E)-avenanthramide D	Phenolic alkaloid	3.666	$C_{16}H_{13}NO_4$	−9.56
6.	cyclohexylamine	Aliphatic amine	3.919	$C_6H_{13}N$	−6.95
7.	L-2-amino-3- methylenehexanoic acid	Amino acid derivative	4.1	$C_7H_{13}NO_2$	−2.63
8.	D-lysine	Amino acid	4.357	$C_6H_{14}N_2O_2$	−3.34
9.	triethylene glycol diglycidyl ether	Epoxy compound	5.082	$C_{12}H_{22}O_6$	3.14
10.	L-isoleucyl-l-proline	Dipeptide	5.266	$C_{11}H_{20}N_2O3$	13.33
11.	methyl N-methylanthranilate	Methyl ester of an anthranilic acid derivative	5.385	$C_9H_{11}NO_2$	−0.43
12.	D-tryptophan	Essential amino acid	5.389	$C_{11}H_{12}N_2O_2$	13.66
13.	phenylethylamine	Biogenic amine	5.459	$C_8H_{11}N$	−2.07
14.	asparaginyl-Gamma- glutamate	Peptide	5.845	$C_9H_{16}N_4O_5$	−1.35
15.	L-alpha-Amino-1H-pyrrole-1- hexanoic acid	Amino acid derivative	5.853	$C_{10}H_{16}N_2O_2$	13.76
16.	tyrosyl-Leucine	Dipeptide	6.094	$C_{15}H_{22}N_2O_4$	14.33
17.	mycinamicin I	Macrolide antibiotic	6.157	$C_{37}H_{61}N\ O_{12}$	−2.36
18.	trans,trans-1,4-Diphenyl-1,3- butadiene	Diene (Conjugated polyene)	6.254	$C_{16}H_{14}$	8.05
19.	(17alpha,23S)-17,23-Epoxy-29- hydroxy-27-norlanosta-1,8- diene-3,15,24-trione	Triterpenoid	7.549	$C_{29}H_{40}O_5$	−6.27
20.	Momordicin II	Triterpenoid saponin	8.964	$C_{36}H_{58}O_9$	12.65
21.	medicagenic acid 3-O-b-d- glucuronide	Triterpenoid glucuronide	8.965	$C_{36}H_{54}O_{12}$	−3.65
22.	goyaglycoside c	Flavonoid glycoside	10.178	$C_{38}H_{62}O_9$	12.87
23.	D-ala-d-Ala	Dipeptide	1.499	$C_6H_{12}N_2O_3$	−2.44
24.	quinic acid	Hydroxycarboxylic acid	1.499	$C_7H_{12}O_6$	−0.72
25.	phenylacetohydroxamic acid	Hydroxamic acid derivative	2.258	$C_8H_9NO_2$	−7.15
26.	(E)-C-HDMAPP	Isoprenoid	2.269	$C_6H_{14}O_7P_2$	−0.35
27.	arabinose uridinemonophosphate	Nucleoside sugar derivative	2.412	$C_9H_{13}N_2O_9P$	−6.62
28.	gallic acid	Phenolic acid	3.952	$C_7H_6O_5$	−2.74
29.	fuca1–2Galβ1–4Glcβ-SP	Glycoside	4.193	$C_{20}H_{35}N_3O_{15}$	8.95
30.	threoninyl valine	Dipeptide	4.281	$C_{19}H_{18}N_2O_4$	−7.46
31.	mebeverine metabolite (veratric acid glucuronide)	Glucuronide conjugate of phenolic acid	4.426	$C_{15}H_{18}O_{10}$	4.86
32.	trans-Zeatin	Cytokinin (Plant hormone)	4.581	$C_{10}H_{13}N_5O$	1.17
33.	ile Glu	Dipeptide	4.75	$C_{11}H_{20}N_2O_5$	−4.31
34.	tyr Phe Tyr	Tripeptide	4.892	$C_{27}H_{29}N_3O_6$	0.89
35.	muconic dialdehyde	Aldehyde derivative	4.949	$C_6H_6O_2$	−2.44
36.	resorcinol	Phenolic compound	4.949	$C_6H_6O_2$	−2.44
37.	gentisic acid	Phenolic acid	4.949	$C_7H_6O_4$	−1.94
38.	lipomycin	Polyketide antibiotic	5.047	$C_{32}H_{45}NO_9$	−7.48
39.	xanthone	Polycyclic aromatic ketone	5.273	$C_{19}H_{14}O_2$	
40.	aspidoalbine	Alkaloid	5.29	$C_{24}H_{32}N_2O_5$	2.33
41.	His Pro	Tripeptide	5.364	$C_{17}H_{23}N_7O_4$	−2.56
42.	(3x,5x,10x)-9,10- Didehydroisohumbertiol O- [rhamnosyl-(1->4)-rhamnosyl-(1->2)-[rhamnosyl-(1->6)]- glucoside]	Flavonoid glycosid	5.381	$C_{39}H_{62}O_{18}$	−5.53
43.	veratridine	Alkaloid	5.95	$C_{36}H_{51}NO_{11}$	−2.19
44.	androcymbine	Alkaloid	6.165	$C_{21}H_{25}N\ O_5$	3.68
45.	PI(P-16:0/22:6(4Z,7Z,10Z,13Z,16Z,19Z))	Phosphatidylinositol (PI) with polyunsaturated fatty acid (PUFA) chains	6.39	$C_{47}H_{79}O_{12}P$	3.17
46.	S-(PGA1)-glutathione	Glutathione conjugate	6.466	$C_{30}H_{49}N_3O_{10}S$	−13.77
47.	11-hydroxyyohimbine	Indole alkaloid	6.467	$C_{21}H_{26}N_2O_4$	5.39
48.	leu Cys Leu	Tripeptide	6.735	$C_{15}H_{29}N_3O_4S$	2.4
49.	capryloylglycine	Fatty acid amide	6.773	$C_{10}H_{19}NO_3$	−0.23
50.	androcymbine	Alkaloid	6.883	$C_{21}H_{25}NO_5$	4.54
51.	6-bromo-pentacosa-5E,9Z-dienoic acid	Fatty acid derivative	6.883	$C_{25}H_{45}BrO_2$	−2.96
52.	hydroxypentobarbital	Barbiturate derivative	6.963	$C_{11}H_{18}N_2O_4$	−7.13
53.	benzoic acid	Aromatic carboxylic acid	7.012	$C_7H_6O_2$	−1.49
54.	cyclolinopeptide H	Cyclopeptide	7.115	$C_{56}H_{75}N_9O_9S_2$	1
55.	calenduloside H	Triterpenoid saponin	7.378	$C_{48}H_{76}O_{19}$	−3.3
56.	PI(O-18:0/0:0)	Phosphoinositide	7.396	$C_{27}H_{55}O_{11}P$	4.79
57.	bluensomycin	Antibiotic (Polyketide)	7.492	$C_{21}H_{39}N_5O_{14}$	−3.75
58.	trp Ile Leu	Tripeptide	7.494	$C_{23}H_{34}N_4O_4$	−7.25
59.	trunkamide A	Peptide	7.737	$C_{43}H_{63}N_7O_8S$	0.4
60.	gln Cys Lys	Tripeptide	7.996	$C_{14}H_{27}N_5O_5S$	−1.55
61.	8′-hydroxydihydroergotamine	Ergot alkaloid derivative	8.22	$C_{33}H_{37}N_5O_6$	13.94
62.	myxochromide S1	Polyketide antibiotic	8.309	$C_{38}H_{54}N_6O_8$	−1.9
63.	pro Tyr Pro	Tripeptide	8.582	$C_{19}H_{25}N_3O_5$	−5.67
64.	licoricesaponin E2	Triterpenoid saponin	8.81	$C_{42}H_{60}O_{16}$	3.15
65.	asn Lys Met	Tripeptide	8.883	$C_{15}H_{29}N_5O_5S$	−1
66.	vignatic acid A	Phenolic acid derivative	8.895	$C_{30}H_{39}N_3O_7$	0.1
67.	pipercide	Alkaloid	9.198	$C_{22}H_{29}NO_3$	3.97
68.	asn Lys Met	Tripeptide	9.215	$C_{15}H_{29}N_5O_5S$	−1.78
69.	PI(18:2(9Z,12Z)/18:4(6Z,9Z, 12Z,15Z))	Phosphoinositide	9.36	$C_{45}H_{75}O_{13}P$	−1.86
70.	Baliospermin	Alkaloid	9.618	$C_{32}H_{50}O_8$	3.62

(*continued on next page*)

Table 5 (*continued*)

Sl. No.	Identified Compound Name	Class of Compounds	RT (min)	Formula	ppm
71.	PS(15:0/18:4(6Z,9Z,12Z,15Z))	Phosphatidylserine (PS)	10.123	$C_{39}H_{68}NO_{10}P$	14.84
72.	congmuyenoside B	Saponin	10.38	$C_{54}H_{88}O_2$	3.23
73.	fucalpha1–2Galbeta1- 3GlcNAcbeta1–3(GlcNAcbeta1- 6) Galbeta1–3GlcNAcbeta1- 3Galbeta1–4Glcbeta-Cer(d18:1/26:1(17Z))	Glycosphingolipid	10.433	$C_{98}H_{174}N_4O_{42}$	15.44
74.	CDP-DG(18:0/18:2(9Z,12Z))	Cytidine diphosphate-diacylglycerol (CDP-DG)	10.657	$C_{48}H_{85}N_3O_{15}P_2$	9.58
75.	N tteuAcalpha2–6Galbeta1- 3GalNAcbeta1–3Galalpha1- 4Galbeta1–4Glcbeta-Cer(d18:1/20:0	Glycosphingolipid (ganglioside)	11.137	$C_{81}H_{145}N_3O_{36}$	5.04
76.	PI(18:3(6Z,9Z,12Z)/17:1(9Z))	Phosphoinositide (phosphatidylinositol)	11.182	$C_{44}H_{77}O_{13}P$	−1.01

Cytotoxic activity (MTT assay)

The cytotoxic effects of the ethyl acetate extract from *B. amyloliquefaciens* on L929 mouse fibroblast cells were assessed through the MTT assay. The results for cell viability were presented as a percentage, comparing treated cells to those in the untreated control group. Across the tested extract volumes (20, 40, 60, 80, and 100 µl), no significant dose-dependent decrease in cell viability was detected (Fig. 17). The highest cytotoxicity was observed at 100 µl of the extract, which resulted in a cell viability of 97.46 %. The results show that at the tested concentrations, *B. amyloliquefaciens* ethyl acetate extract has no harmful effects on L929 fibroblast cells. (Fig. 16).

Discussion

The current study aims on isolation, identification, and characterization of an endophytic bacterial strain from *P. chaba* which have antibacterial, antioxidant, and antibiofilm properties. Previous studies on *P. chaba* have predominantly focused on the isolation and characterization of endophytic fungi with antibacterial potential, while endophytic bacterial communities remain largely unexplored (Gouda et al., 2016).

Surface-sterilized samples of *P. chaba* roots, stems, fruits, and leaves yielded 40 bacterial isolates, confirming the presence of diverse endophytic communities within different plant tissues. The effectiveness of the sterilization protocol was validated by the absence of microbial growth on control plates, ensuring that only true endophytes were recovered. This approach aligns well with previous studies that employed sodium hypochlorite and ethanol for surface sterilization, successfully isolating endophytes from various plant tissues (Xie et al., 2021).

The differential distribution of endophytic bacteria across various plant parts suggests potential tissue-specific colonization patterns. Such variations may be attributed to differences in nutrient availability, plant defence mechanisms, or environmental factors within the host tissues. The predominance of Gram-positive bacteria aligns with previous studies that report Gram positive bacteria (39 out of 40 isolates) aligns to prior studies that report Gram positive bacteria particularly *Bacillus* and *Actinobacteria*, as dominant endophytes due to their stress tolerance and ability to establish a symbiotic relationship with plants (Chen et al., 2019). These findings provide a foundational understanding of the endophytic bacterial diversity in *P. chaba*, paving the way for further characterization of their functional roles and secondary metabolite production (Mossie, 2024).

Among the isolates, PLS06 demonstrated remarkable antibacterial activity against ESBL producing *K. pneumoniae* and was identified as *B. amyloliquefaciens* NWR-14 through 16S rRNA sequencing. This finding aligns well with the work of Liao et al. (2024), who reported the potent antibacterial properties of endophytic *B. amyloliquefaciens* isolated from a variety of medicinal plants. Their study highlighted its efficacy against antibiotic-resistant pathogens, reinforcing the potential of endophytic bacteria as an alternative strategy to combat antimicrobial resistance. Further, Arifiyanto et al. (2023) demonstrated that endophytic bacteria isolated from nutmeg exhibited antibacterial activity against *Escherichia coli*, suggesting that diverse plant-associated bacteria possess broad-spectrum antimicrobial properties.

A *Bacillus* endophyte isolated from peanut roots showed the production of effective antimicrobial compounds against *Ralstonia solanacearum* and *Aspergillus flavus* (Chen et al., 2019). Liao et al. (2024) reported the isolation of bacterial endophytes with antibacterial activity from the traditional medicinal plant *Crinum macowanii*. These endophytes exhibited antibacterial activity against five bacterial pathogens: *E. coli, Pseudomonas aeruginosa, K. pneumoniae, Staphylococcus aureus*, and *Bacillus cereus*. Studies by Khan et al. (2014) and others have shown similar outcomes, underscoring the potential of endophytic microbial strains from medicinal plants as important sources of antimicrobial compounds.

The increase in antibiotic resistance among pathogenic microorganisms is a significant obstacle that reduces the available treatment options (Anh et al., 2022). In addition to clinical pathogens, environmental strains of bacteria also frequently carry antibiotic-resistant genes, which can spread horizontally to other microorganisms and exacerbate the resistance crisis (Christina et al., 2013). To analyze the resistance patterns and possible clinical significance of the isolated endophytic bacteria, the antibiotic susceptibility profiles of these bacteria were evaluated using 14 distinct antibiotics. The antibiotics were selected to represent a broad spectrum of antibacterial activity, including inhibitors of cell wall synthesis (penicillin, ampicillin, imipenem, bacitracin), protein synthesis (tetracycline, erythromycin, amikacin, gentamicin, chloramphenicol), and nucleic acid synthesis (ciprofloxacin, nalidixic acid, levofloxacin, norfloxacin). This selection ensures coverage of clinically relevant antibiotics and those commonly encountered in environmental microbiology and agriculture. The strain demonstrated sensitivity to broad-spectrum antibiotics, such as ciprofloxacin and imipenem, suggesting that these antibiotics could be considered in combination therapies for treating infections involving these strains. Furthermore, B. amyloliquefaciens NWR-14 exhibited a multiple antibiotic resistance (MAR) index of 42 %, indicating resistance to several antibiotic classes. While this may reflect moderate antibiotic pressure in its native environment, such a resistance profile also raises important biosafety concerns. Although some studies suggest that resistance in non-pathogenic strains may reduce the risk of horizontal gene transfer to pathogenic bacteria, this interpretation remains speculative in the absence of genomic data. Therefore, comprehensive genomic characterization is required to assess the underlying resistance mechanisms, environmental adaptation, and the overall safety and therapeutic potential of the strain (Atta et al., 2023).

The endophytic *B. amyloliquefaciens* NWR-14 used in this study exhibited no hemolytic activity, indicating its safety for potential biotechnological, probiotic, and medical applications. This result is crucial, as hemolysin production can pose risks when considering bacterial strains for therapeutic or industrial use. Prior research has underscored the need to evaluate the hemolytic characteristics of *Bacillus* strains to confirm their appropriateness. Liao et al. (2024) compared the hemolytic properties of various *B. amyloliquefaciens* strains, highlighting the necessity of selecting non-hemolytic strains for

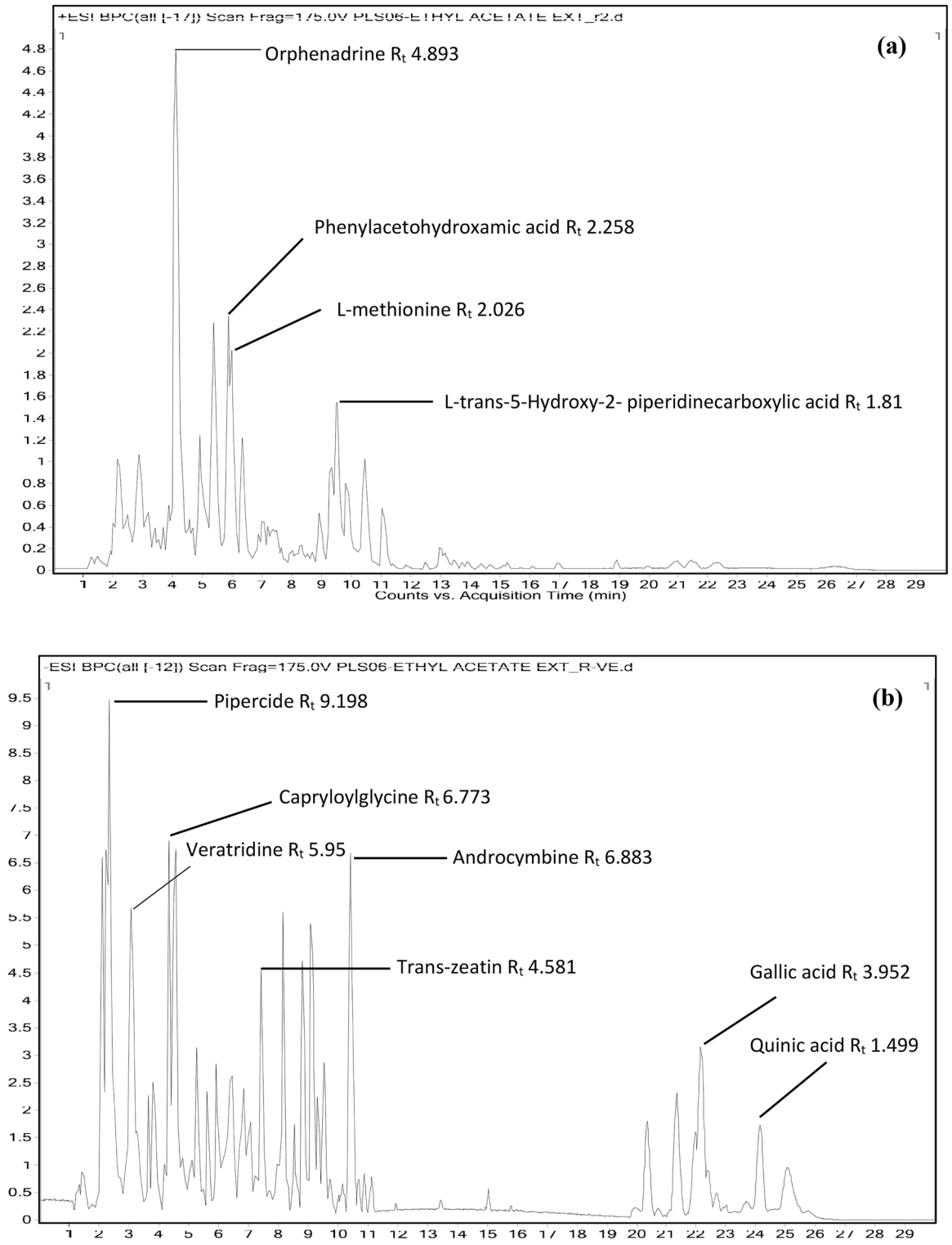

Fig. 14. Bioactive compounds annotatedin the ethyl acetate extract of *B. amyloliquifaciens*using the HR-LCMS technique. (**a**) ESI positive mode (**b**) ESI negative mode.

probiotic applications. Similarly, Xie et al. (2021) underscored the need for thorough safety assessments before utilizing *Bacillus* strains in human and animal health. Some strains may produce hemolysins under specific environmental conditions, as Dabire et al. (2022) demonstrated that hemolysin production varies based on strain type and cultivation conditions. Furthermore, another study screened 76 Bacillus strains and identified six non-hemolytic strains deemed safe for human and animal applications. Our findings align with these reports, reinforcing the need for strain-specific safety evaluations when considering B. amyloliquefaciens for industrial or clinical applications (Christina et al., 2013).

Previous studies have demonstrated that ethyl acetate is an effective solvent for extracting bioactive compounds with antibacterial properties from *Bacillus* species (Xie et al., 2021). In our study, the ethyl acetate extract of *B. amyloliquefaciens* exhibited the most potent antibacterial

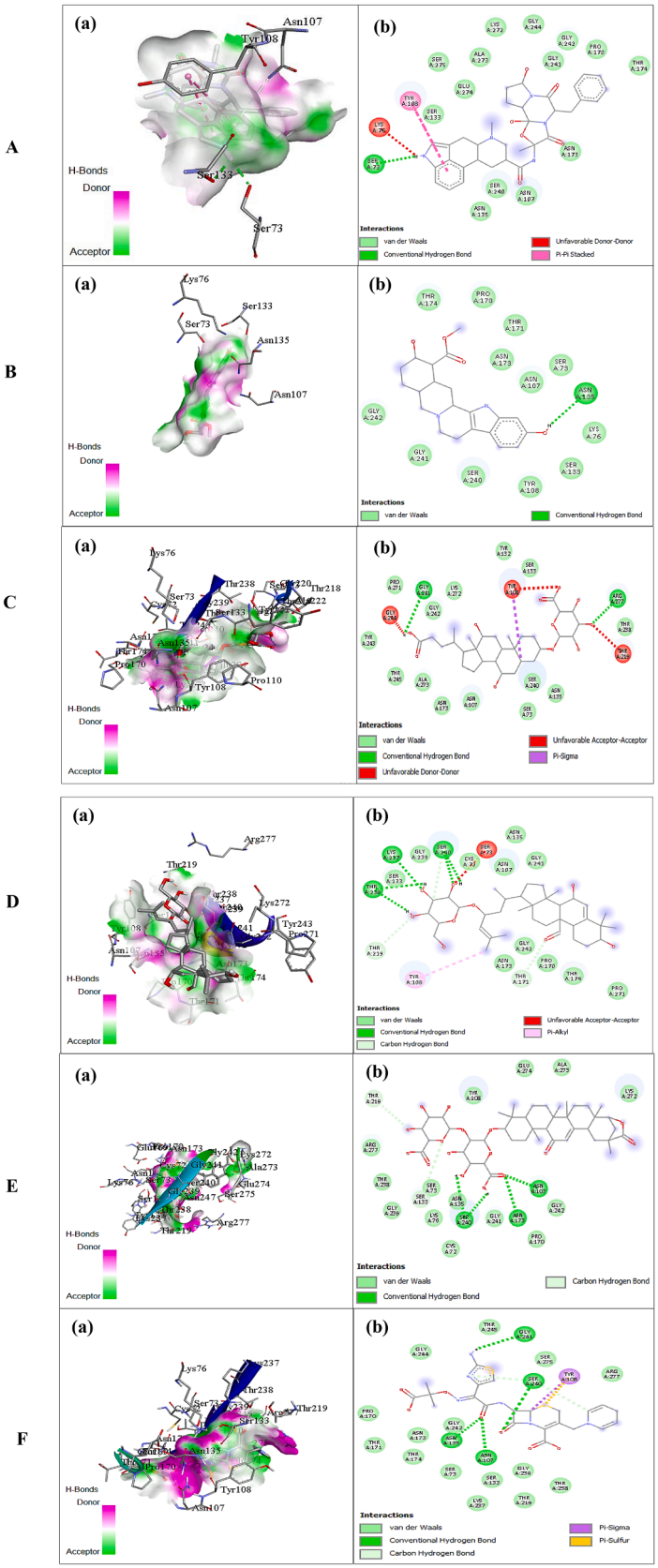

Fig. 15. (**a**) 3D and (**b**) 2D binding interactions of selected compounds exhibiting strong binding affinities with the CTX-M-15 active site (PDB ID: 5T66).The compounds include: A –8′-Hydroxydihydroergotamine, B –11-Hydroxyyohimbine, C –Cholic acid glucuronide, D –Momordicin II, E –Licoricesaponin E2, and F –positive control (Ceftazidime–clavulanic acid).

Table 6
Antioxidant activity of the ethyl acetate extract of *B. amyloliquefaciens* and standard ascorbic acid determined by DPPH, FRAP, and ABTS assays.

Assay	Sample	Absorbance @ 0.5 (μg/ml or μl)	IC_{50} (μg/ml or μl)	Interpretation
DPPH assay	*B. amyloliquefaciens* extract	365.428 μg/ml	170.795 μg/ml	Moderate antioxidant activity
	Ascorbic acid (positive control)	37.379 μg/ml	10.462 μg/ml	Strong antioxidant activity
FRAP assay	*B. amyloliquefaciens* extract	365.428 μg/ml ($A = 0.5$)	–	Low reducing power
	Ascorbic acid	37.379 μg/ml ($A = 0.5$)	–	High reducing power
ABTS assay	*B. amyloliquefaciens* extract	–	200.34 μl	Moderate antioxidant activity
	Ascorbic acid	–	15.99 μg/ml	Strong antioxidant activity

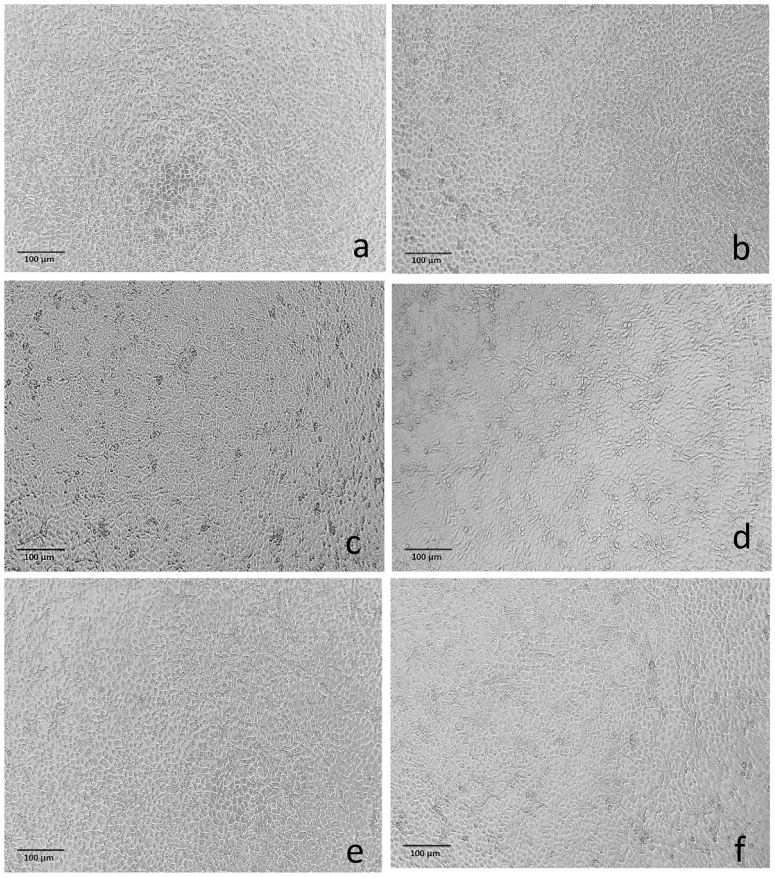

Fig. 16. Cell lines with different concentrations: **a** – Control, **b** – 20 μl, **c** – 40 μl, **d** – 60 μl, **e** – 80 μl, **f** – 100 μl.

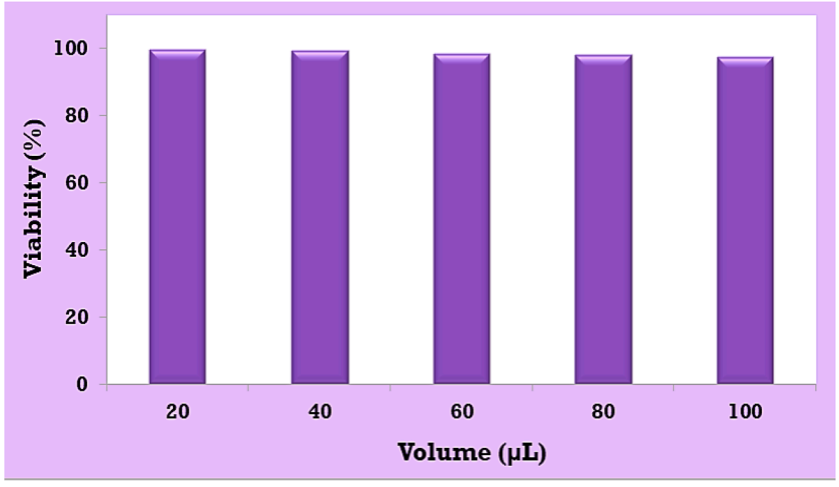

Fig. 17. Cell viability of L929 cells treated with ethyl acetate extract of *B. amyloliquefaciens*.

activity against *K. pneumoniae*, followed by the butanol extract. These findings highlight the crucial role of solvent selection in determining the antimicrobial efficacy of bacterial extracts.

The ethyl acetate extract of B. amyloliquefaciens exhibited moderate antibacterial activity, with MIC and MBC values of 1.56 mg/mL**,** as per established classification guidelines (Xie et al., 2021). While antibiofilm activity was observed at concentrations of 3 mg/ml and 6 mg/ml. These findings correspond with previous studies indicating that ethyl acetate fractions contain multiple antibacterial compounds that disrupt bacterial metabolic pathways and inhibit cell division by compromising the stability of the bacterial cell membrane. Importantly, this mode of action is less frequently linked to bacterial resistance, making it a promising alternative to conventional antibiotics (Agrawal et al., 2021). Additionally, our results suggest that the active compounds in the extract predominantly target the bacterial cell surface, potentially compromising membrane integrity. Since biofilm-associated infections are particularly challenging to treat due to their resistance to standard therapies (Asokan et al., 2025), the extract's ability to prevent biofilm formation underscores its potential clinical significance. This highlights its promise as a viable candidate for addressing biofilm-related infections, which remain a major concern in healthcare.

The MIC and MBC values fall into a moderate activity range, according to established classification thresholds for crude natural product extracts. For instance, MICs between 0.5–1.0 mg/ml are considered moderate, while values between 1.0–2.0 mg/ml indicate low antimicrobial activity (Mossie, 2024). Such concentrations are common for unrefined plant and microbial extracts, where active compounds exist in low abundance within complex mixtures. These findings support the significance of our results while also highlighting the necessity of bioactivity-guided fractionation (Nephali et al., 2022) to isolate and concentrate the active constituents, potentially leading to improved potency.

The ethyl acetate extract demonstrated dose-dependent biofilm inhibition against K. pneumoniae. However, the antibiofilm effects were observed only at relatively high concentrations, indicating moderate efficacy**.** Notably, this is typical for crude extracts, and their activity can often be significantly enhanced through bioactivity-guided fractionation or by combining them with antibiotic methods proven to reduce MICs and enhance biofilm disruption (Atta et al. 2023). For example, synergy assays with Thymbra spicata extracts and various antibiotics (ampicillin, cefotaxime, amikacin) against multidrug-resistant K. pneumoniae showed fractional inhibitory concentration indices of 0.25–0.50, indicating clear synergistic interactions that improve antibacterial effectiveness beyond the extract alone (Haroun and Al-Kayali, 2016; Hemaiswarya et al., 2008).

SEM revealed significant morphological alterations in K. pneumoniae cells treated with the crude extract of B. amyloliquefaciens NWR-14, including membrane deformation, surface blebbing, and cellular collapse features indicative of structural damage. These observations suggest that the bioactive compounds may interfere with membrane integrity, potentially leading to cell lysis. Similar ultrastructural damage has been reported in K. pneumoniae following exposure to bioactive plant and microbial extracts (Agrawal et al., 2021). They also demonstrated membrane rupture and crater-like lesions in *E. coli* upon treatment with antimicrobial peptides, even in the absence of biochemical membrane assays. Additionally, surface blebbing and collapse visualized by SEM and TEM were associated with polymyxin B and colistin treatment in *E. coli* (Liao et al., 2024), supporting the interpretation of membrane-targeting activity based on morphological criteria. While the SEM findings in our study are consistent with membrane disruption, further mechanistic investigations are required to confirm this mode of action.

The annotated metabolites were cross-referenced with the Human Metabolome Database (HMDB). Out of the 76 annotated compounds, 54 were successfully matched with HMDB IDs, while 22 compounds did not have corresponding entries. The complete list of annotations, including retention time, observed *m/z*, ppm error, molecular formula, and HMDB identifiers, is provided in Supplementary Table S3. Several of the identified compounds have previously been reported in Bacillus species, endophytic bacteria, or microbial communities associated with Piperaceae, thereby strengthening the biological and ecological significance of our findings. Fatty acids such as oleic acid (cis-9-octadecenoic acid) and n-hexadecanoic acid (palmitic acid), also annotated in the present study, are widely reported in bacterial metabolomes and were previously observed in Piper-associated endophytic communities. Additionally, compounds such as dihydrocapsaicin and β-homoproline (3-aminopropanoic acid) were reported in Piper betel endophyte extracts and were similarly detected in our strain. These overlapping metabolites suggest potential metabolic convergence between endophytic bacteria and their host plants, possibly facilitated by co-evolution or horizontal gene transfer (Nephali et al., 2022; Cushnie et al., 2014).

The ecological relevance of these findings is supported by recent studies emphasizing the holobiont concept, wherein metabolite profiles of host plants and their microbiota often mirror each other due to genetic exchange and shared biosynthetic pathways. Dabire et al. (2022) highlighted the role of horizontal gene transfer in shaping microbial secondary metabolism within plant-associated environments. In this context, the presence of phytochemically relevant compounds in the B. amyloliquefaciens NWR-14 extract may reflect its long-term adaptation within the P. chaba host. Beyond known microbial metabolites, our analysis also annotated biologically significant compounds, including 3-methyl sulfolene, Mycinamicin I, and Momordicin II each reported in literature for their antimicrobial, antioxidant, or anti-inflammatory properties. These findings are consistent with earlier reports that B. amyloliquefaciens exhibits substantial metabolic versatility, particularly in producing polyketides (e.g., macrolactin, bacillaene, difficidin), ribosomal peptides (e.g., mersacidin), and cyclic lipopeptides (e.g., iturin, surfactin, fengycin), all of which possess well-documented antimicrobial and biocontrol activities (Jiao et al., 2021). Taken together, the results highlight B. amyloliquefaciens NWR-14 as a promising source of bioactive secondary metabolites with potential therapeutic applications. Its metabolite profile supports its use in the development of antibacterial agents targeting multidrug-resistant pathogens. Future research should aim to purify individual metabolites, investigate their mechanisms of action, and optimize their production for pharmaceutical use.

Bioactive compounds derived from *B. amyloliquefaciens* NWR-14 exhibit promising inhibitory potential against CTX-M-15, a key enzyme mediating β-lactam resistance in *K. pneumoniae.* Notably, 8′-hydroxydihydroergotamine displayed the highest binding affinity (−8.8 kcal/mol), surpassing known inhibitors such as avibactam (∼−7.5 kcal/mol) and tazobactam (−6.5 to −7.0 kcal/mol). This exceptional binding suggests its potential as a next-generation β-lactamase inhibitor, possibly overcoming the limitations of current therapeutics (Jamil et al., 2023; Drawz et al., 2010).

Another strong compound, licoricesaponin E2 (−8.2 kcal/mol), a saponin with documented antimicrobial properties, likely inhibits CTX-M-15 by targeting critical residues like Ser70, thereby impeding β-lactam hydrolysis. Similarly, 11-hydroxyyohimbine (−8.1 kcal/mol) demonstrated strong binding interactions, consistent with previous studies that highlight plant-derived alkaloids as effective β-lactamase inhibitors. For comparison, berberine, an alkaloid from *Berberis* species exhibits binding energies of −7.0 to −7.5 kcal/mol [81], suggesting that these compounds may offer comparable or superior efficacy. While androcymbine (−6.4 kcal/mol) and aspidoalbine (−6.4 kcal/mol) showed moderate affinities, they could still contribute to combination therapies, a strategy proven to rejuvenate β-lactam activity against resistant pathogens (Degfie et al., 2022).

Additional compounds such as d-tryptophan, and trans-zeatin (all with binding energies of −6.0 kcal/mol) demonstrated comparatively lower affinity for CTX-M-15. While these molecules may exhibit limited standalone inhibitory activity, they could play a valuable role in synergistic combinations with other antimicrobial agents, consistent with

polypharmacological approaches to boost treatment outcomes. These findings correlate with existing research on natural β-lactamase inhibitors. Notably, epigallocatechin gallate (EGCG) from green tea shows CTX-M-15 inhibition (−7.2 kcal/mol), and curcumin (from turmeric) exhibits activity against ESBLs (−6.5 to −7.0 kcal/mol). The discovery of compounds with exceptional binding affinities (below −8.0 kcal/mol) points to a novel class of potent inhibitors that could potentially surpass current natural alternatives in combating β-lactam resistance (Degfie et al., 2022).

The ethyl acetate extract from *B. amyloliquefaciens* NWR-14 exhibited significant antioxidant activity, with an IC50 value of 170.795 µg/ml in the DPPH assay. Although less potent than ascorbic acid, a standard antioxidant, its free radical scavenging potential highlights its therapeutic relevance in oxidative stress-related disorders. These findings reinforce previous reports identifying *B. amyloliquefaciens* as a promising source of antioxidant compounds (Shahzad et al., 2020). Antioxidant properties in *B. amyloliquefaciens* have been observed across diverse environments. Shahzad et al. (2020) demonstrated that endophytic *B. amyloliquefaciens* RWL-1 enhanced antioxidant activity in fermented soybean. The consistent antioxidant activity observed across studies highlights *Bacillus* species' pharmaceutical and probiotic potential. The antioxidant activity of *B. amyloliquefaciens* NWR-14 suggests a valuable source of bioactive metabolites for therapeutic development. However, further research is needed to characterize the specific compounds responsible for this activity and elucidate their mechanisms of action.

The MTT assay revealed the non-cytotoxic nature of the ethyl acetate extract from *B. amyloliquefaciens* NWR-14 against L929 fibroblast cells, even at higher concentrations. This finding suggests a favourable safety profile, a critical factor for therapeutic applications. The results are consistent with the earlier research showing that metabolites from *Bacillus* have low toxicity to mammalian cells, supporting their promise as antimicrobial agents (Harwood et al., 2018). The low cytotoxicity of *B. amyloliquefaciens* metabolites is well-documented. For instance, Harwood et al. (2018) demonstrated that antimicrobial *Bacillus* secondary metabolites show negligible toxicity in mammalian models, supporting their clinical applicability. Likewise, studies on *B. subtilis* and *B. amyloliquefaciens* have shown that lipopeptides and polyketides selectively target pathogens while sparing host cells, a key attribute for safe therapeutic use (Jiao et al., 2021). The absence of cytotoxicity in our study, combined with existing literature, underscores the therapeutic potential of *B. amyloliquefaciens* NWR-14 metabolites, particularly in the face of rising antimicrobial resistance.

While HR-LCMS facilitated broad profiling of secondary metabolites, this study has two main analytical limitations. First, metabolite identifications were based solely on accurate mass and retention time, without MS/MS-based structural confirmation. As such, the annotations remain putative and require validation through tandem mass spectrometry and comparison with authentic standards. Second, due to the unavailability of HPLC-UV instrumentation, classical chromatographic fingerprinting and quantification of marker compounds could not be performed. Instead, total ion chromatograms were used to represent the extract's chemical profile. Future investigations should incorporate validated HPLC-UV methods and MS/MS analyses to strengthen compound identification, improve standardization, and enhance reproducibility in extract-based studies.

Conclusion

This study demonstrates the bioactive potential of B. amyloliquefaciens NWR-14, an endophytic bacterium isolated from P. chaba, which exhibited antimicrobial, antioxidant, and antibiofilm activities. The ethyl acetate extract showed inhibitory effects against multidrug-resistant K. pneumoniae, supported by morphological damage observed through SEM analysis. HR-LCMS profiling putatively annotated several compounds with known pharmacological relevance, and molecular docking indicated potential interactions with the CTX-M-15 resistance enzyme. The results underscore the contribution of endophytic bacteria as valuable sources of secondary metabolites with therapeutic relevance and strengthen the rationale for their inclusion in antimicrobial screening studies.

Funding

The research did not receive any specific grant from funding agencies in the public, commercial or non-profit sectors.

Ethical approval

The study protocol was ethically approved by the Institutional Review Board (No: IRB/03/10/2023) of Pushpagiri Institute of Medical Sciences & Research Centre, Tiruvalla, Kerala, India.

Informed consent

Not applicable

Data availability

Data will be made available on request.

CRediT authorship contribution statement

Sijo Asokan: Writing – original draft, Visualization, Methodology, Investigation, Data curation. **Teena Jacob:** Supervision, Methodology, Formal analysis. **Tijo Cherian:** Methodology, Formal analysis. **Teena Merlin:** Methodology, Formal analysis. **Vivekanandhan S:** Methodology. **Afaf A AlSosowaa:** Software. **Mostafa Mohammed Atiyah:** Formal analysis. **Faheem Q Al-Mojahid:** Formal analysis. **Willie J.G.M. Peijnenburg:** Formal analysis. **Smitha Vijayan:** Writing – review & editing, Validation, Supervision, Project administration, Methodology, Conceptualization.

Declaration of competing interest

The authors declare that they have no known competing financial interests or personal relationships that could have appeared to influence the work reported in this paper.

Acknowledgements

We thank the School of Biosciences, MACFAST College, for providing the necessary facilities to conduct this research. We also thank the Clinical Microbiology Laboratory at Pushpagiri Medical College Hospital for providing the clinical strains of ESBL-producing *K. pneumoniae*. We sincerely appreciate the Pharmacognosy Unit of the Regional Ayurveda Research Institute (RARI), Poojappura, Trivandrum District, Kerala, for supplying the *Piper chaba* plant material used in this study. We are deeply grateful to the Principal Scientist at JNTBGRI, Palode, Trivandrum, Kerala, for their expertise in identifying the plant, verifying the specimen, and incorporating it into the herbarium collection. We also acknowledge the Regional Facility for DNA Fingerprinting (RFDF) at the Rajiv Gandhi Centre for Biotechnology (RGCB), Trivandrum, Kerala, for conducting the 16S rRNA gene sequencing, which was crucial to our research. Furthermore, we express our appreciation to the SAIF facility at the Indian Institute of Technology (IIT), Mumbai, India, for facilitating the HR-LCMS analysis, which significantly contributed to the findings of this study.

Supplementary materials

Supplementary material associated with this article can be found, in the online version, at doi:10.1016/j.phyplu.2025.100885.

References

Agrawal, S., Nandeibam, J., Sarangthem, I., 2021. Ultrastructural changes in methicillin-resistant *Staphylococcus aureus* (MRSA) induced by metabolites of thermophilous fungi *Acrophialophora levis*. PLoS. One 16, e0258607. https://doi.org/10.1371/journal.pone.0258607. –e0258607.

Anh, H.T.L., Linh, B.N.H., Dung, N.H.T., Minh, D.D., Le Quyen, T.T., Trung, T.T., 2022. In vitro safety evaluation of *Bacillus subtilis* species complex isolated from Vietnam and their additional beneficial properties. Vietnam J. Biotechnol. 20, 727–740.

Arifiyanto, A., Farisi, S., 2023. Antioxidant activity of endophytic bacteria isolated from *Pyrrosia piloselloides* (L.) M.G. Price. Baghdad Sci. J. 20.

Aswani, P., Tijith, K., George, Jisha, M.S, 2017. Characterization of bioactive metabolites of endophytic *Fusarium solani* isolated from *Withania somnifera*. J. Biol. Act. Prod. Nat. 7, 411–426.

Atta, S., Waseem, D., Fatima, H., Naz, I., Rasheed, F., Kanwal, N., 2023. Antibacterial potential and synergistic interaction between natural polyphenolic extracts and synthetic antibiotic on clinical isolates. Saudi. J. Biol. Sci. 30, 103576. –103576.

Bush, K., 2018. Past and present perspectives on β-lactamases. Antimicrob. Agents Chemother 62, e01076. https://doi.org/10.1128/AAC.01076-18. –18.

Asokan, S., Jacob, T., Jacob, J., AlSosowaa, A.A., Vijayan, S., 2025a. Trends in antimicrobial susceptibility patterns of *Klebsiella pneumoniae* isolated from clinical samples at a tertiary care hospital in Kerala, India. Next Res., 100654

Chen, L., Shi, H., Heng, J., Wang, D., Bian, K., 2019. Antimicrobial, plant growth-promoting and genomic properties of the peanut endophyte *Bacillus velezensis* LDO2. Microbiol. Res. 218, 41–48.

Christina, A., Christapher, V., Bhore, S.J., 2013. Endophytic bacteria as a source of novel antibiotics: an overview. Pharmacogn. Rev. 7, 11–16.

Cushnie, T.T., Cushnie, B., Lamb, A.J., 2014. Alkaloids: an overview of their antibacterial, antibiotic-enhancing and antivirulence activities. Int. J. Antimicrob. Agents 44, 377–386.

Dabiré, Y., Somda, N.S., Somda, M.K., Mogmenga, I., Traoré, A.K., Ezeogu, L.I., 2022. Molecular identification and safety assessment of *Bacillus* strains isolated from Burkinabe traditional condiment "soumbala. Ann. Microbiol. 72, 10. https://doi.org/10.1186/s13213-021-01673-w. –10.

Degfie, T., Endale, M., Tafese, T., Dekebo, A., Shenkute, K., 2022. In vitro antibacterial, antioxidant activities, molecular docking, and ADMET analysis of phytochemicals from roots of *Hydnora johannis*. Appl. Biol. Chem. 65, 76. –76.

Asokan, S., Jacob, T., Jacob, J., AlSosowaa, A.A., Cherian, T., Peijnenburg, W.J., Vijayan, S., 2025b. Klebsiella pneumoniae: a growing threat in the era of antimicrobial resistance. The Microbe, 100333.

Drawz, S.M., Bonomo, R.A., 2010. Three decades of β-lactamase inhibitors. Clin. Microbiol. Rev. 23, 160–201.

Gouda, S., Das, G., Sen, S.K., Shin, H.-S., Patra, J.K., 2016. Endophytes: a treasure house of bioactive compounds of medicinal importance. Front. Microbiol. 7, 1538. https://doi.org/10.3389/fmicb.2016.01538. –1538.

Haroun, M.F., Al-Kayali, R.S., 2016. Synergistic effect of *Thymbra spicata* L. extracts with antibiotics against multidrug-resistant *Staphylococcus aureus* and *Klebsiella pneumoniae* strains. Iran. J. Basic Med. Sci. 19, 1193–1199.

Harwood, C.R., Mouillon, J.M., Pohl, S., Arnau, J., 2018. Secondary metabolite production and the safety of industrially important members of the *Bacillus subtilis* group. FEMS Microbiol. Rev. 42, 721–738. https://doi.org/10.1093/femsre/fuy012.

Hemaiswarya, S., Kruthiventi, A.K., Doble, M., 2008. Synergism between natural products and antibiotics against infectious diseases. Phytomedicine 15, 639–652.

Islam, M.T., Hasan, J., Snigdha, H.S.H., Ali, E.S., Sharifi-Rad, J., Martorell, M., Mubarak, M.S., 2020. Chemical profile, traditional uses, and biological activities of *Piper chaba* Hunter: a review. J. Ethnopharmacol. 257, 112853. https://doi.org/10.1016/j.jep.2020.112853. –112853.

Jamil, F., Zahra, N.U.A., Uddin, R., 2023. Construction of a comprehensive protein-protein interaction map for multidrug-resistant *Klebsiella pneumoniae* to identify drug targets: a computational approach. Pak. J. Pharm. Sci. 36, 129–148.

Jiao, R., Cai, Y., He, P., Munir, S., Li, X., Wu, Y., 2021. *Bacillus amyloliquefaciens* YN201732 produces lipopeptides with promising biocontrol activity against fungal pathogen *Erysiphe cichoracearum*. Front. Cell Infect. Microbiol. 11, 598999. –598999.

Khan, A.L., Waqas, M., Kang, S.-M., Al-Harrasi, A., Hussain, J., Al-Rawahi, A., 2014. Bacterial endophyte *Sphingomonas* sp. LK11 produces gibberellins and IAA and promotes tomato plant growth. J. Microbiol. 52, 689–695. https://doi.org/10.1007/s12275-014-4002-7.

Liao, J., Chen, Y., Lin, Y., Wei, J., Gao, H., Liu, Y., Gu, W., Xie, Z., Zhou, S., 2024. Comparison of antibacterial activities of six *Bacillus amyloliquefaciens* strains. J. Clin. Nurs. Res. 8, 261–272. https://doi.org/10.26689/jcnr.v8i9.8353.

Litao, N., Rustamova, N., Paerhati, P., Ning, H.X., Yili, A., 2023. Culturable diversity and biological properties of bacterial endophytes associated with the medicinal plants of *Vernonia anthelmintica* (L.) Willd. Appl. Sci. 13, 9797. –9797.

Mekky, A.E., Farrag, A.A., Hmed, A.A., Sofy, A.R., 2021. Preparation of zinc oxide nanoparticles using *Aspergillus niger* as antimicrobial and anticancer agents. J. Pure Appl. Microbiol. 15, 1547–1566.

Mengistu, A.A., 2020. Endophytes: colonization, behaviour, and their role in defense mechanism. Int. J. Microbiol. 2020, 6927219. https://doi.org/10.1155/2020/6927219. –6927219.

Monowar, T., Rahman, M.S., Bhore, S.J., Raju, G., Sathasivam, K.V., 2018. Silver nanoparticles synthesized by using the endophytic bacterium *Pantoea ananatis* are promising antimicrobial agents against multidrug resistant bacteria. Molecules. 23, 3220. –3220.

Mosmann, T., 1983. Rapid colorimetric assay for cellular growth and survival: application to proliferation and cytotoxicity assays. J. Immunol. Methods 65, 55–63.

Mossie, T., 2024. In vitro antibacterial activity of *Bersama abyssinica* Fresen crude extract against representative Gram-positive and Gram-negative bacterial isolates. Vet. Med. Sci. 10, e1498. –e1498.

Nephali, L., Steenkamp, P., Burgess, K., Huyser, J., Brand, M., van der Hooft, J.J., Tugizimana, F., 2022. Mass spectral molecular networking to profile the metabolome of biostimulant *Bacillus* strains. Front. Plant Sci. 13, 920963.

Nisa, S., Khan, N., Shah, W., Sabir, M., Khan, W., Bibi, Y., 2020. Identification and bioactivities of two endophytic fungi *Fusarium fujikuroi* and *Aspergillus tubingensis* from foliar parts of *Debregeasia salicifolia*. Arab. J. Sci. Eng. 45, 1–11. https://doi.org/10.1007/s13369-020-04454-1.

Sansinenea, E., Vaca, J., Rojas, N.E., Vázquez, C., 2020. A wide spectrum of antibacterial activity of secondary metabolites from *Bacillus amyloliquefaciens* ELI149. Biosci. J. 36, 235–244.

Shahzad, R., Shehzad, A., Bilal, S., Lee, I.J., 2020. *Bacillus amyloliquefaciens* RWL-1 as a new potential strain for augmenting biochemical and nutritional composition of fermented soybean. Molecules. 25, 2346. https://doi.org/10.3390/molecules25102346. –2346.

Vijayan, S., Divya, K., Varghese, S., Jisha, M.S., 2020. Antifungal efficacy of chitosan-stabilized biogenic silver nanoparticles against pathogenic *Candida* spp. isolated from human. Bionanoscience 10, 974–982.

Xie, Y., Peng, Q., Ji, Y., Xie, A., Yang, L., Mu, S., 2021. Isolation and identification of antibacterial bioactive compounds from *Bacillus megaterium* L2. Front. Microbiol. 12, 645484. https://doi.org/10.3389/fmicb.2021.645484. –645484.